Presynaptic $G\alpha_o$ (GOA-1) signals to depress command neuron excitability and allow stretch-dependent modulation of egg laying in *Caenorhabditis elegans*

Bhavya Ravi[1,2,3], Jian Zhao[4,5], Sana Chaudhry[2], Mattingly Bartole[1,2], Richard J. Kopchock 3rd [2], Christian Guijarro[2,6], Lijun Kang[4], and Kevin M. Collins[1,2,7]

[1]Neuroscience Program, University of Miami Miller School of Medicine, Miami, FL USA

[2]Department of Biology, University of Miami, Coral Gables, FL USA

[3]Present address: Department of Neurology, Johns Hopkins University School of Medicine, Baltimore, MD USA

[4]Department of Neuroscience, Zhejiang University School of Medicine, Hangzhou, Zhejiang, China

[5]Present address: Department of Molecular Biology, Massachusetts General Hospital, Boston, MA USA

[6]Present address: ALPS Electric Europe GmbH, Munich, Germany

[7]To whom correspondence should be addressed:

kevin.collins@miami.edu

Department of Biology
University of Miami
1301 Memorial Drive
Coral Gables, FL 33143
Tel: (305) 284-9058

Short title: Presynaptic $G\alpha_o$ inhibits command neuron excitability

54 pages with 7 Figures, 2 Tables, and 7 Videos

Abstract- 205 words, Introduction- 648 words, Discussion- 1483 words.

Abstract

Egg laying in the nematode worm *Caenorhabditis elegans* is a two-state behavior modulated by internal and external sensory input. We have previously shown that homeostatic feedback of embryo accumulation in the uterus regulates bursting activity of the serotonergic HSN command neurons that sustains the egg-laying active state. How sensory feedback of egg release signals to terminate the egg-laying active state is less understood. We find that $G\alpha_o$, a conserved Pertussis Toxin-sensitive G protein, signals within HSN to inhibit egg-laying circuit activity and prevent entry into the active state. $G\alpha_o$ signaling hyperpolarizes HSN, reducing HSN Ca^{2+} activity and input onto the postsynaptic vulval muscles. Loss of inhibitory $G\alpha_o$ signaling uncouples presynaptic HSN activity from a postsynaptic, stretch-dependent homeostat, causing precocious entry into the egg-laying active state when only a few eggs are present in the uterus. Feedback of vulval opening and egg release activates the uv1 neuroendocrine cells which release NLP-7 neuropeptides which signal to inhibit egg laying through $G\alpha_o$-independent mechanisms in the HSNs and $G\alpha_o$-dependent mechanisms in cells other than the HSNs. Thus, neuropeptide and inhibitory $G\alpha_o$ signaling maintains a bi-stable state of electrical excitability that dynamically controls circuit activity in response to both external and internal sensory input to drive a two-state behavior output.

Introduction

A major goal of neuroscience is to understand how sensory signals control neural circuit activity and changes in animal behavior. Such sensory feedback informs when a behavior should begin, how long it should continue, and when it should end. Extensive evidence has shown that neuromodulators like serotonin and neuropeptides signal through G protein coupled receptors to remodel neural circuit activity and drive behavior state transitions (Jiang et al., 2001; Goulding et al., 2008). Yet, there is no neural circuit in any organism for which we know precisely how each signaling event contributes to sensory modulation of a behavior. Small neural circuits typically found in invertebrates combine anatomical simplicity with genetic and experimental accessibility, allowing for a complete understanding of the molecular and physiological basis for a behavioral output (Marder, 2012).

The *C. elegans* female egg-laying behavior circuit is ideally suited to study how sensory signals modulate circuit functions that underlie decision-making. As shown in Figure 1A, the circuit is comprised of two Hermaphrodite Specific Neurons (HSNs) that synapse onto the egg-laying vulval muscles (White et al., 1986; Shen et al., 2004; Li et al., 2013). During ~2 minute active states, rhythmic HSN Ca^{2+} activity releases serotonin and neuropeptides that signal to promote the excitability of the muscles, driving ejection of ~4-6 eggs in sequence from the uterus into the environment (Waggoner et al., 1998; Shyn et al., 2003; Zhang et al., 2008; Collins et al., 2016; Brewer et al., 2019). External and internal sensory input regulate the onset of egg laying (Horvitz et al., 1982; Trent, 1982; Sawin, 1996; Aprison and Ruvinsky, 2014; Ravi et al., 2018a), and genetic studies have identified neuropeptides, receptors, and two antagonistic heterotrimeric G proteins that signal to regulate HSN activity, neurotransmitter release, and egg laying (Schafer, 2006; Koelle, 2016). $G\alpha_q$ signals through the conserved PLCβ and Trio RhoGEF effector pathways to promote neurotransmitter release and egg laying (Brundage et

71 al., 1996; Lackner et al., 1999; Miller et al., 1999; Bastiani et al., 2003; McMullan et al., 2006;
72 Williams et al., 2007; McMullan and Nurrish, 2011). Because phorbol ester DAG-mimetics such
73 as PMA rescue synaptic transmission defects of $G\alpha_q$ signaling mutants (Lackner et al., 1999;
74 Williams et al., 2007), DAG production and recruitment of UNC-13 and/or Protein Kinase C
75 effectors is thought to mediate the $G\alpha_q$ dependent modulation of synaptic transmission (Yawo,
76 1999; Wierda et al., 2007; Lou et al., 2008). $G\alpha_q$ signaling is opposed by $G\alpha_o$ which signals to
77 inhibit neurotransmitter release (Koelle and Horvitz, 1996; Miller et al., 1999; Nurrish et al.,
78 1999), vulval muscle activity (Shyn et al., 2003), and egg laying (Mendel et al., 1995; Segalat et
79 al., 1995). How $G\alpha_o$ signaling antagonizes $G\alpha_q$, Rho, and DAG signaling is not clear. Even
80 though $G\alpha_o$ mediates signaling by numerous neurotransmitters in diverse animals including
81 mammals (Jiang et al., 2001), direct effectors for $G\alpha_o$ have not yet been identified. In *C.*
82 *elegans*, $G\alpha_o$ mutants resemble animals lacking DAG Kinase; both mutants show increased
83 UNC-13 localization to synapses and hyperactive egg-laying behavior defects, resembling
84 treatment with phorbol esters (Miller et al., 1999; Nurrish et al., 1999; Jose and Koelle, 2005).
85 Because synaptic transmission could be modulated by upstream changes in cell and circuit
86 electrical excitability and/or by downstream effects on synaptic vesicle fusion, what is needed
87 are direct measurements of how discrete changes in G protein and effector signaling affect cell
88 and circuit activity and their consequences on animal behavior.

89 Here we explore how $G\alpha_o$ inhibits *C. elegans* egg-laying circuit activity and behavior.
90 Our data reveal that $G\alpha_o$ signaling reduces the electrical excitability of the HSN command
91 neurons to promote the inactive state while eggs are produced. Feedback of egg accumulation
92 in the uterus then switches the circuit into active states where rhythmic bursting drives
93 sequential egg-laying events. Thus, modulation by inhibitory $G\alpha_o$ signaling allows for proper

94 induction of motor behavior circuit upon the alignment of optimal external and internal sensory
95 conditions.

96

97 **Results**

98 **Reduced inhibitory Gα$_o$ signaling leads to premature egg laying and decreases the**
99 **duration of egg-laying inactive states**

100 To better understand how inhibitory Gα$_o$ signaling contributes to egg-laying behavior
101 state transitions, we used mutants and transgenes to manipulate Gα$_o$ signaling in specific cells
102 of the egg-laying circuit and analyzed the consequences on cell Ca^{2+} activity and behavior. We
103 found that Gα$_o$ signaling inhibits the onset of egg laying. We performed a 'time to first egg lay'
104 assay in wild-type animals and in mutants with excessive or reduced Gα$_o$ signaling. As
105 previously shown, wild-type animals release their first embryo ~6-7 hours after becoming
106 adults (McMullen et al., 2012; Ravi et al., 2018a). Animals bearing Gα$_o$ loss-of-function or null
107 mutations laid their eggs much earlier, 3-4 hours after becoming adults (Figure 1B). *goa-*
108 *1(n1134)*, a hypomorphic mutant predicted to lack the conserved N-terminal myristoylation and
109 palmitoylation sequence, and *goa-1(sa734)*, an early stop mutant predicted to be a molecular
110 null (Segalat et al., 1995; Robatzek and Thomas, 2000), showed similarly precocious onset of egg
111 laying (Figure 1B). This phenotype was shared in transgenic animals where Gα$_o$ function was
112 inhibited just in HSNs through the cell-specific expression of Pertussis Toxin (Tanis et al.,
113 2008). Because the timing of this first egg-laying event requires serotonin along with HSN
114 function and activity (Ravi et al., 2018a), these results suggest that Gα$_o$ normally signals in HSN
115 to inhibit neurotransmitter release and thereby delay the first egg-laying active state (Figure

116 1B). To test the effects of increased $G\alpha_o$ signaling, we analyzed the behavior of *egl-10(md176)*
117 mutants which lack the major RGS protein that terminates $G\alpha_o$ signaling by promoting $G\alpha_o$
118 GTP hydrolysis (Koelle and Horvitz, 1996). *egl-10(md176)* mutants showed a strong and
119 significant delay in the onset of egg laying, laying their first egg ~15 hours after reaching
120 adulthood (Figure 1B). This delay of egg-laying phenotype was shared in transgenic animals
121 expressing the constitutively active $G\alpha_o$ (Q205L) mutant specifically in the HSNs (Tanis et al.,
122 2008) and resembled animals developmentally lacking HSNs (Ravi et al., 2018a), consistent
123 with $G\alpha_o$ signaling in HSN to inhibit neurotransmitter release that normally drives the onset of
124 egg laying.

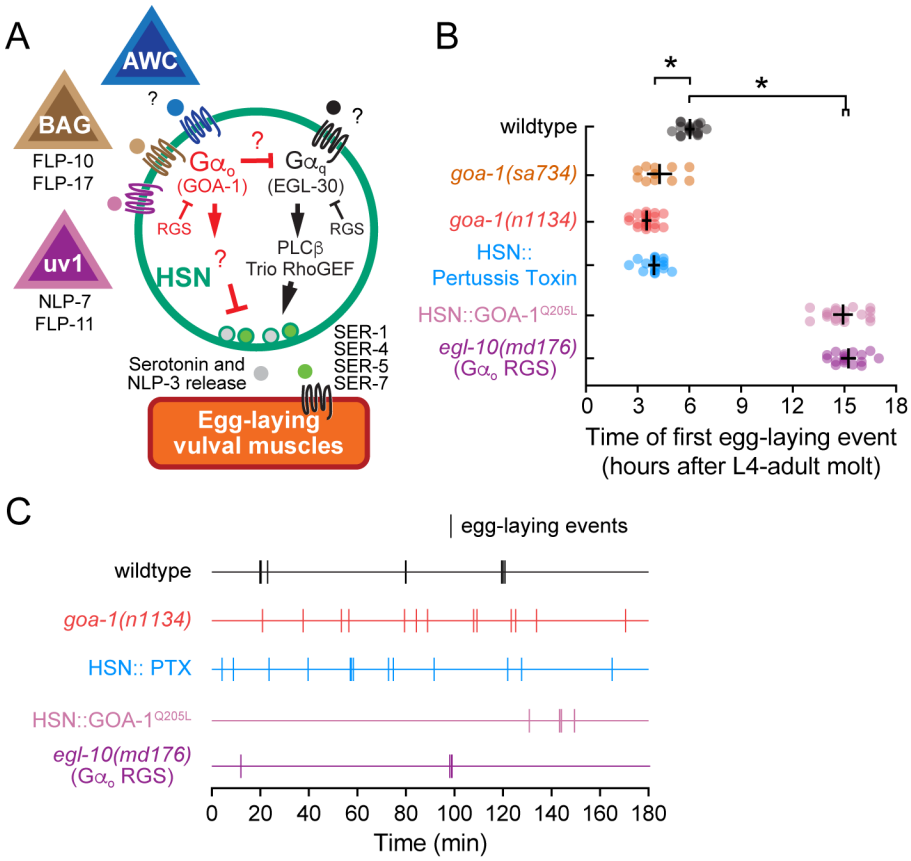

125

126 **Figure 1. $G\alpha_o$ signaling maintains the inactive egg-laying behavior state.**
127 (**A**) Cartoon of how identified and unidentified neuropeptides released from AWC (Fenk and de
128 Bono, 2015), BAG (Ringstad and Horvitz, 2008), uv1 (Banerjee et al., 2017), and other sensory
129 cells bind to G-protein coupled receptors expressed on HSN command neurons (green) which

130 signal via $G\alpha_o$ (red) or $G\alpha_q$ (black) effector pathways to modulate serotonin and NLP-3
131 neuropeptide release (Tanis et al., 2008; Brewer et al., 2019). The egg-laying vulval muscles
132 (orange) express receptors for serotonin (Carnell et al., 2005; Dempsey et al., 2005; Hobson et
133 al., 2006; Fernandez et al., 2020) and possibly NLP-3 which signal to promote vulval muscle
134 excitability and egg laying (**B**) Scatter plots of the first egg-laying event in wildtype (grey), null
135 *goa-1(sa734)* mutants (orange), hypomorphic loss-of-function *goa-1(n1134)* mutants (red), *egl-*
136 *10(md176)* null mutants (purple), and transgenic animals expressing Pertussis Toxin (blue) or
137 GOA-1^{Q205L} in the HSNs (pink). Error bars show 95% confidence intervals for the mean from
138 ≥10 animals. Asterisks indicate p≤0.0001 (One-way ANOVA with Bonferroni correction for
139 multiple comparisons). (**C**) Representative raster plots showing temporal pattern of egg laying
140 during three hours in wild-type (black), hypomorphic loss-of-function *goa-1(n1134)* mutant
141 (red), and *egl-10(md176)* null mutant animals (purple), along with transgenic animals
142 expressing Pertussis Toxin (blue) or GOA-1^{Q205L} in the HSNs (pink). Vertical lines indicate
143 single egg-laying events.

144

145 To understand how $G\alpha_o$ signaling controls the normal two-state pattern of egg laying,
146 we performed long-term recordings of adults as they transitioned into and out of the active
147 states in which clusters of several eggs are typically laid. We defined intra-cluster intervals as
148 the time elapsed between consecutive egg-laying events within a single active state (e.g.
149 intervals < 4 minutes) and inter-cluster intervals as the time elapsed between different active
150 states (e.g. intervals > 4 minutes), as described (Waggoner et al., 1998; Collins and Koelle,
151 2013). As expected, wild-type animals displayed a two-state pattern of egg laying with multiple
152 egg-laying events clustered within brief, ~2-minute active states about every 20-30 minutes
153 (Figure 1C and Table 1). Animals bearing the *goa-1(n1134)* hypomorphic mutation entered
154 active states 2-3-fold more frequently, often laying single eggs during active states separated
155 by only ~12-13 minutes (Figure 1C and Table 1), as previously shown (Waggoner et al., 2000).
156 We found the duration of inactive states in animals expressing Pertussis Toxin in the HSN
157 neurons was indistinguishable from the *goa-1(n1134)* mutant, indicating that $G\alpha_o$ signals in
158 HSN to reduce the probability of entering the active state (Figure 1C and Table 1). Loss of
159 inhibitory $G\alpha_o$ signaling led to active states in which 1-2 embryos were laid almost immediately
160 after they were positioned in the uterus next to the vulval opening. As a result, successive egg-
161 laying events were rate-limited by egg production, explaining why the average intra-cluster

162 intervals were typically double seen in wild-type animals (Figure 1C and Table 1). Conversely,
163 *egl-10(md176)* mutant animals or transgenic animals expressing the $G\alpha_o$(Q205L) gain-of-
164 function mutation in the HSNs showed prolonged inactive periods of 258 and 67 min,
165 respectively (Figure 1C and Table 1), resembling animals lacking HSNs altogether (Waggoner
166 et al., 2000). Interestingly, animals without HSNs or with too much inhibitory $G\alpha_o$ signaling still
167 lay multiple eggs within discrete active states (Figure 1C and Table 1), consistent with our
168 results showing that a stretch-dependent homeostat can maintain the active state even when
169 neurotransmitter release from the HSN is inhibited (Collins et al., 2016; Ravi et al., 2018a).
170 These results show that $G\alpha_o$ signaling does not modulate patterns of egg laying within active
171 states. Instead, $G\alpha_o$ acts in HSN to depress entry into the egg-laying active state.

	***Intra*-cluster interval ($1/\lambda_1$)**	***Inter*-cluster interval ($1/\lambda_2$)**	**Eggs laid per active state**	**Unlaid eggs per animal**
Genotype	**Average (min) (95%CI range)**	**Average (min) (95%CI range)**	**Average ± 95%CI**	**Average ± 95%CI**
Wild type	0.42 (0.33-0.51)	22.11 (21.19-23.09)	2.5 ± 0.5	15.9 ± 1.5
goa-1(n1134)	1.31 (0.94-1.67)	12.88* (12.31-12.75)	1.2 ± 0.1‡	2.2 ± 0.3
HSN::Pertussis Toxin	1.69 (1.17-2.20)	12.42* (12.09-12.75)	1.1 ± 0.07‡	4.1 ± 0.3#
egl-10(md176)	0.64 (0.49-0.79)	258.6* (231.26-293.42)	2.5 ± 0.2	45.9 ± 3.3
HSN::GOA-1^{Q205L}	0.35 (0.24-0.47)	66.97* (64.14-70.02)	2.2 ± 0.2	36.8 ± 3.8

172 **Table 1. Egg-laying behavior measurements in animals with altered $G\alpha_o$ signaling.**

173 Long-term behavior recordings were used to extract features of egg-laying active and inactive
174 behavior states for the indicated genotypes, as described (Waggoner et al., 1998). '*' indicates
175 significant differences compared to wild-type animals (p<0.0001, Kruskal-Wallis test with
176 Dunn's correction for multiple comparisons), '‡' indicates significant differences compared to

177 wildtype ($p<0.0001$, One-way ANOVA with Bonferroni correction), and '#' indicates that this
178 result was previously reported (Tanis et al., 2008).

179

180 **$G\alpha_o$ signaling inhibits HSN Ca^{2+} activity to promote the inactive behavior state**

181 Previous work has shown that $G\alpha_o$ signals presnaptically to depress neurotransmitter
182 release. Whether $G\alpha_o$ signals to inhibit HSN electrical excitability that might be evident in
183 changes in cell Ca^{2+} activity, or instead signals downstream of Ca^{2+} to regulate steps in UNC-
184 13-dependent docking, priming, and vesicle fusion, has not been tested directly. To address
185 how $G\alpha_o$ signals to inhibit HSN neurotransmitter release, we performed ratiometric Ca^{2+}
186 imaging in our panel of $G\alpha_o$ signaling mutants as they entered spontaneous egg-laying active
187 states. Freely behaving animals bearing the *goa-1(n1134)* hypomorphic or *goa-1(sa734)* null
188 mutations showed a clear change in HSN Ca^{2+} activity from two-state burst firing to more tonic
189 firing (Figure 2A, Videos 1-3). Complete loss of inhibitory $G\alpha_o$ signaling caused a significant
190 increase in the frequency of HSN Ca^{2+} transients (Figure 2B and 2C). We were surprised that
191 the *goa-1(n1134)* mutants, which show strongly hyperactive egg-laying behavior
192 indistinguishable from that of *goa-1(sa734)* null mutants, showed only a modest and
193 statistically insignificant increase in HSN Ca^{2+} activity compared to wild-type (Figure 2C).
194 However, our results with *goa-1(n1134)* match previously findings (Shyn et al., 2003). The *goa-*
195 *1(n1134)* hypomorphic mutant is expected to have residual $G\alpha_o$ signaling activity in that its
196 major defect is the absence of a proper membrane anchor sequence (Mumby et al., 1990).
197 These results show that $G\alpha_o$ signaling depresses HSN presynaptic activity, but that the
198 hyperactive egg-laying phenotypes observed in *goa-1(n1134)* mutants are separable from an
199 increase in presynaptic HSN Ca^{2+} activity.

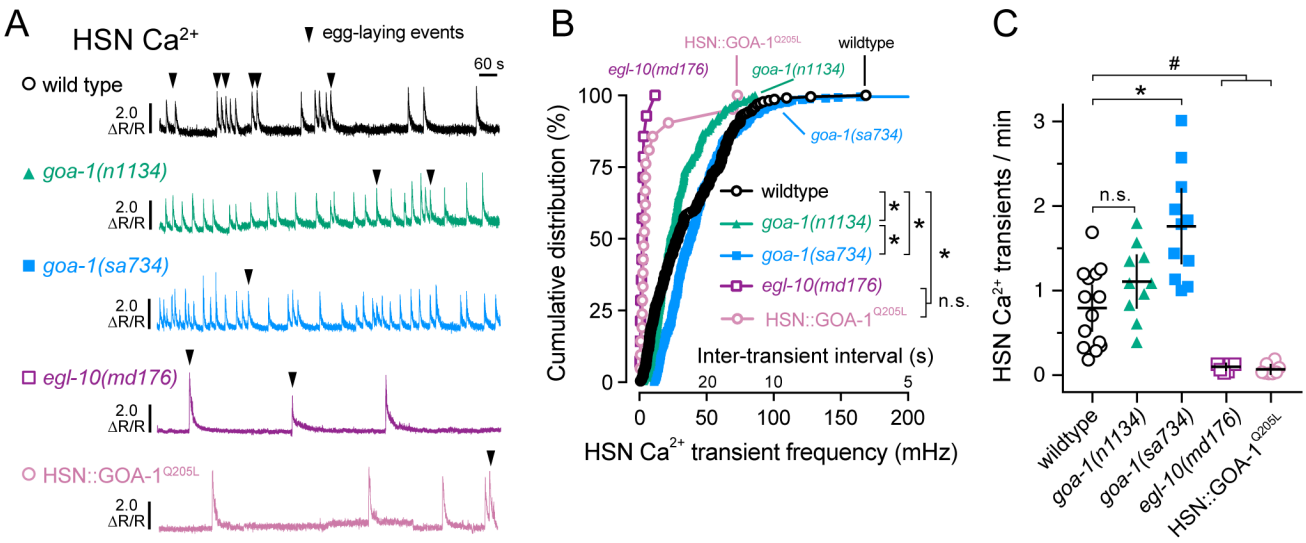

Figure 2. Gα$_o$ signaling inhibits HSN neuron Ca^{2+} activity and burst firing.

(**A**) Representative GCaMP5:mCherry (ΔR/R) ratio traces showing HSN Ca^{2+} activity in freely behaving wild-type (black), *goa-1(n1134)* loss-of-function mutant (green), *goa-1(sa734)* null mutant (blue), and *egl-10(md176)* null (purple) mutant animals, along with transgenic animals expressing the activated GOA-1(Q205L) in the HSN neurons (pink) during an egg-laying active state. Arrowheads indicate egg-laying events. (**B**) Cumulative distribution plots of instantaneous Ca^{2+} transient peak frequencies (and inter-transient intervals) in wild-type (black open circles), *goa-1(n1134)* (green filled triangles), *goa-1(sa734)* (blue squares), *egl-10(md176)* mutants (purple open squares) along with transgenic animals expressing the activated GOA-1(Q205L) in the HSN neurons (pink open circles). Asterisks indicate $p<0.0001$ (Kruskal-Wallis test with Dunn's correction for multiple comparisons). (**C**) Scatter plots show average Ca^{2+} transient frequency (per min). Error bars indicate 95% confidence intervals for the mean. Asterisk indicates $p<0.0001$; pound (#) indicates $p\leq0.0079$; n.s. indicates $p>0.05$ (One-way ANOVA with Bonferroni correction for multiple comparisons).

We next tested how increased inhibitory Gα$_o$ signaling affects HSN activity. Both *egl-10(md176)* mutants and transgenic animals expressing the activated GOA-1(Q205L) in HSNs showed a significant and dramatic reduction in the frequency of HSN Ca^{2+} transients, with single HSN Ca^{2+} transients occuring several minutes apart (Figure 2A and 2B). The rare egg-laying events seen in animals with increased Gα$_o$ signaling mostly followed single HSN Ca^{2+} transients, not multi-transient bursts typically seen in wild-type animals (Figure 2A and 2C). In one *egl-10(md176)* animal, we observed an egg-laying event that was not accompanied by an

223 HSN Ca^{2+} transient. This suggests that elevated $G\alpha_o$ signaling is sufficient to silence the
224 HSNs, and that, in this case, egg laying becomes HSN-independent. In support of this model,
225 previous work has shown that *egl-10(md176)* mutants respond to serotonin but are resistant to
226 the serotonin reuptake inhibitor imipramine (Trent et al., 1983). Alternatively (or additionally)
227 $G\alpha_o$ signaling may function to depress coordinated activity between the gap-junctioned,
228 contralateral HSNs, whose Ca^{2+} activity we were unable to observe simultaneously because
229 our confocal imaging conditions only captures one HSN at a time.

230 To determine how disruption of inhibitory $G\alpha_o$ signaling in HSN affects its activity, we
231 recorded HSN Ca^{2+} transients in transgenic animals expressing Pertussis Toxin in the HSNs.
232 $G\alpha_o$-silenced HSNs showed a dramatic increase in the frequency of HSN Ca^{2+} transients,
233 leading to a nearly constitutive, tonic Ca^{2+} activity like that observed in *goa-1(sa734)* null
234 mutants (Figure 3A, 3B, and 3C; Video 4). While control animals showed an average HSN
235 Ca^{2+} transient frequency of about ~0.4 transients per minute, animals expressing Pertussis
236 Toxin in HSN showed an average 1.9 transients per minute, a significant increase (Figure 3C).
237 These results suggest that even under normal growth conditions, unidentified neuromodulators
238 signal through $G\alpha_o$-coupled receptors on HSN to inhibit Ca^{2+} activity. We hypothesize that the
239 observed changes in presynaptic UNC-13 localization (Nurrish et al., 1999) and serotonin
240 biosynthesis (Tanis et al. 2008) when inhibitory $G\alpha_o$ signaling is reduced are consequences,
241 not causes, of altered presynaptic activity.

242

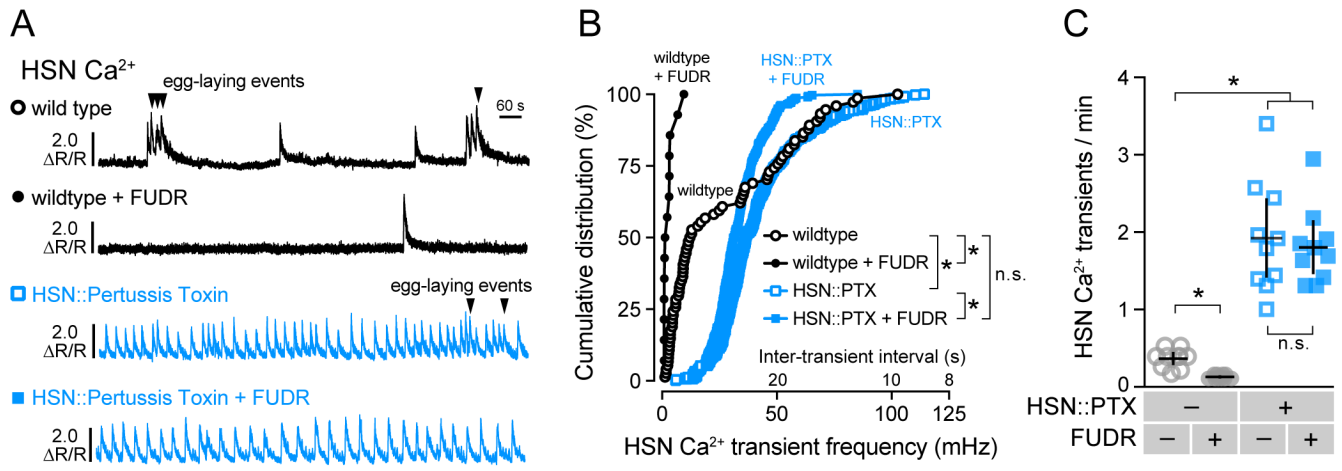

Figure 3. Inhibitory Gα$_o$ signaling in HSN is required for two-state Ca^{2+} activity and facilitates modulation by feedback of egg accumulation.

(A) Representative GCaMP5:mCherry (ΔR/R) ratio traces showing HSN Ca^{2+} activity in untreated (fertile) wild-type animals (black open circles), FUDR-sterilized wild-type animals (black filled circles), untreated (fertile) animals expressing Pertussis Toxin (PTX) in the HSN neurons (blue open squares), and in FUDR-sterilized transgenic animals expressing PTX in the HSNs (blue filled squares). Arrowheads indicate egg-laying events. (**B**) Cumulative distribution plots of instantaneous Ca^{2+} transient peak frequencies (and inter-transient intervals) in untreated and FUDR-treated animals. Asterisks indicate $p<0.0001$ (Kruskal-Wallis test with Dunn's test for multiple comparisons). (**C**) Scatter plots show average Ca^{2+} transient frequency (per min). Error bars indicate 95% confidence intervals for the mean. Asterisks indicate $p<0.0001$ (One-way ANOVA with Bonferroni's test for multiple comparisons). Data from 10 animals were used for each strain for analysis.

We have previously shown that burst Ca^{2+} activity in the command HSN neurons is initiated and sustained by a stretch-dependent homeostat. In chemically or genetically sterilized animals, burst Ca^{2+} activity in HSN is largely eliminated (Ravi et al., 2018a). As such, we were surprised to observe high frequency Ca^{2+} transients in animals with reduced Gα$_o$ signaling because these animals typically retain few (1 to 3) eggs in the uterus at steady state, conditions that normally eliminate HSN burst firing. We hypothesized that the stretch-dependent homeostat was not required to promote HSN Ca^{2+} activity in Gα$_o$ signaling mutants. To test this, we chemically sterilized transgenic animals expressing Pertussis Toxin in the HSNs with Floxuridine (FUDR), a blocker of embryogenesis (Mitchell et al., 1979), and

recorded HSN Ca^{2+} activity. Wild-type animals treated with FUDR showed a dramatic decrease in the frequency of HSN Ca^{2+} activity and an elimination of burst firing (Figures 3A-C), as we have previously shown (Ravi et al., 2018a). Sterilized transgenic animals expressing Pertussis Toxin in the HSNs showed only a slight reduction in HSN Ca^{2+} frequency (Figure 3A and 3B). Both fertile and sterile Pertussis Toxin-expressing animals had dramatically and significantly increased HSN Ca^{2+} transient frequency (~1.9 / min), indicating their HSNs no longer responded to the retrograde signals of egg accumulation arising from the stretch-homeostat. One explanation for this result could be that in fertile wild-type animals, feedback of egg accumulation elevates HSN excitability above a firing threshold that overcomes endogenous inhibitory $G\alpha_o$ signaling. Together, these results support a model where $G\alpha_o$ signals in HSN to depress cell electrical excitability which allows for the proper two-state pattern of HSN Ca^{2+} activity that responds to homeostatic feedback of egg accumulation.

Presynaptic $G\alpha_o$ signaling inhibits postsynaptic vulval muscle activity

To test how changes in inhibitory $G\alpha_o$ signaling affect the postsynaptic vulval muscles, we recorded Ca^{2+} activity in the vulval muscles of *goa-1(n1134)* mutant and Pertussis Toxin expressing transgenic animals. Both wild-type and *goa-1(n1134)* mutants showed increased vulval muscle Ca^{2+} transients as the animals entered the egg-laying active state (Figure 4A and 4B). *goa-1(n1134)* mutants also showed elevated muscle activity compared to wild-type control animals during inactive states when no eggs were laid (Figure 4A and 4B), as previously shown (Shyn et al., 2003). Surprisingly, Ca^{2+} activity during egg-laying active states was not significantly different in *goa-1(n1134)* mutant animals (Figure 4A and 4B; compare Videos 5 and 6), a result consistent with $G\alpha_o$ signaling primarily to prolong the inactive state.

These results suggest $G\alpha_o$ signals to inhibit circuit activity during the egg-laying inactive state and/or that loss of $G\alpha_o$ elevates circuit activity that prolongs the active state beyond the brief ~2-3 minute window during which eggs are typically laid (Waggoner et al., 1998). Recordings of vulval muscle Ca^{2+} activity in transgenic animals expressing Pertussis Toxin in the presynaptic HSNs show a dramatic and significant increase in vulval muscle Ca^{2+} transient frequency during both active and inactive states (Figure 4C and 4D; Video 7), confirming $G\alpha_o$ is required in HSN to inhibit neurotransmitter release.

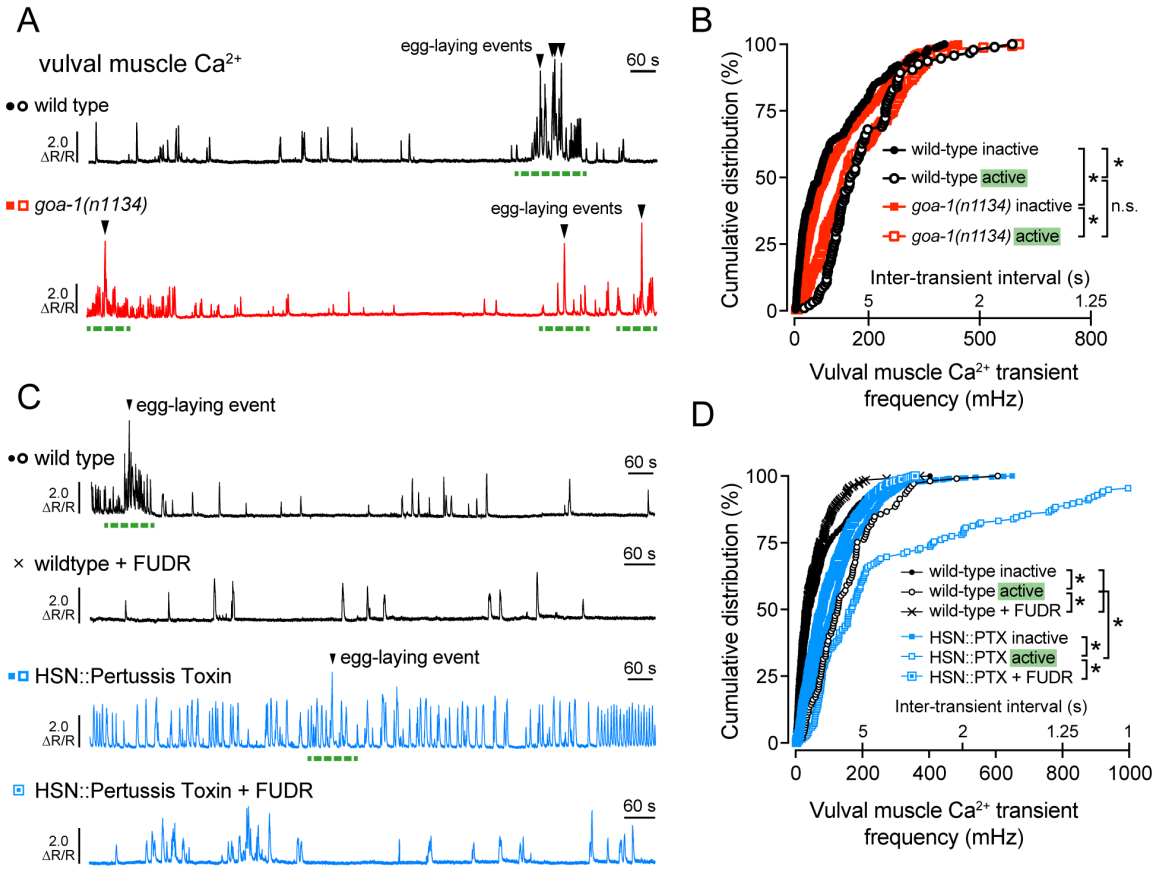

Figure 4. $G\alpha_o$ signals in HSN to reduce excitatory modulation of the vulval muscles.

(A) Representative GCaMP5:mCherry (ΔR/R) ratio traces showing vulval muscle Ca^{2+} activity in wild-type (black) and *goa-1(n1134)* loss-of-function mutant animals (red). Egg-laying events are indicated by arrowheads, and egg-laying active states are indicated by dashed green lines. **(B)** Cumulative distribution plots of instantaneous vulval muscle Ca^{2+} transient peak frequencies (and inter-transient intervals) in wild-type (black circles) and *goa-1(n1134)* mutant animals (red squares) in the inactive and active egg-laying states (filled and open, respectively). **(C)** Representative GCaMP5:mCherry (ΔR/R) ratio traces showing vulval muscle

306 Ca^{2+} activity in untreated (circles) and FUDR-treated (cross) wild-type animals (black) along
307 with untreated (filled) or FUDR-treated (open) transgenic animals expressing Pertussis Toxin
308 in the HSNs (blue squares). Egg-laying events are indicated by arrowheads, and egg-laying
309 active states are indicated by green dashed lines. **(D)** Cumulative distribution plots of
310 instantaneous vulval muscle Ca^{2+} transient peak frequencies (and inter-transient intervals) in
311 wildtype and in transgenic animals expressing Pertussis Toxin in the HSN neurons, with or
312 without FUDR treatment (black cross or blue square), during the inactive and active egg-laying
313 states (filled and open, respectively). Asterisks indicate $p<0.0001$ (Kruskal-Wallis test with
314 Dunn's test for multiple comparisons).

315

316 We have previously shown that egg accumulation promotes vulval muscle excitability
317 during the active state while sterilization reduces it to that seen during the inactive state
318 (Collins et al., 2016; Ravi et al., 2018a). Because FUDR-sterilization failed to reduce HSN Ca^{2+}
319 activity in Pertussis Toxin expressing animals (Figure 3C), we predicted that vulval muscle
320 Ca^{2+} activity would remain similarly elevated in these animals after sterilization. To our
321 surprise, FUDR treatment significantly reduced, but did not completely eliminate, the elevated
322 vulval muscle Ca^{2+} activity in animals expressing Pertussis Toxin in HSN (Figure 4C and 4D).
323 This result suggests egg accumulation and/or germline activity is still required for full vulval
324 muscle activity even when HSN Ca^{2+} activity is dramatically increased. However, because
325 these animals lay eggs almost as soon as they are made, the degree of uterine stretch
326 necessary to induce the active state must be markedly reduced. This supports a model where
327 both the stretch-dependent homeostat and $G\alpha_o$ signaling dynamically interact to regulate egg-
328 laying behavior states.

329

330 **$G\alpha_o$ signaling modulates the HSN resting membrane potential**

331 Reduction of inhibitory $G\alpha_o$ signaling strongly increased HSN Ca^{2+} activity and burst
332 firing, prompting us to investigate whether $G\alpha_o$ signals to modulate HSN electrical excitability.

333 We recorded the resting membrane potential of the HSN neurons in animals with altered $G\alpha_o$
334 signaling using the whole-cell patch clamp technique (Figure 5A), as described (Yue et al.,
335 2018). Hypomorphic *goa-1(n1134)* loss-of-function mutants displayed a trend towards more
336 depolarized resting potentials (-17.9 mV) compared to HSNs from recorded wild-type animals
337 (-21.1 mV), but this difference was not statistically significant (Figure 5B). In contrast, the
338 resting membrane potential of HSNs in *egl-10(md176)* $G\alpha_o$ RGS protein mutant animals with a
339 global increase in $G\alpha_o$ signaling (Koelle and Horvitz, 1996) was significantly hyperpolarized (-
340 40.8 mV) compared to wild-type control animals. This hyperpolarization of HSNs in *egl-*
341 *10(md176)* mutants explains the reduced frequency of HSN Ca^{2+} transients and their strong
342 defects in egg-laying behavior. Transgenic animals expressing Pertussis Toxin specifically in
343 the HSNs had significantly depolarized HSNs (-14.75 mV) compared to the wild-type parental
344 strain (-21.8 mV). These results show that $G\alpha_o$ signals in the HSNs to promote membrane
345 polarization, reducing cell electrical excitability, Ca^{2+} activity, and neurotransmitter release.

346

347 **Inhibition of egg laying by $G\alpha_o$ is not replicated by elevated $\beta\gamma$ expression**

348 Receptor activation of $G\alpha_{i/o}$ heterotrimers releases $\beta\gamma$ subunits which have previously
349 been shown to bind to activate specific K^+ channels and inhibit Ca^{2+} channels (Reuveny et al.,
350 1994; Herlitze et al., 1996). RNAi-mediated knockdown of the GPB-1 β subunit in HSN reduces
351 egg-laying behavior (Esposito et al., 2007). An increase in free $\beta\gamma$ subunits in $G\alpha_o$ mutants
352 might explain their hyperactive egg-laying behavior phenotypes. To test if $\beta\gamma$ over-expression
353 in HSN would increase egg laying, we transgenically overexpressed the sole non-RGS $G\beta$
354 subunit, GPB-1 (Jansen et al., 1999), and the broadly expressed $G\gamma$ subunit, GPC-2 (Yamada et
355 al., 2009), under the *tph-1* promoter along with GFP. $\beta\gamma$ over-expression in HSN did not cause

356 any significant differences in steady-state egg accumulation (Figure 5C). The number of eggs
357 stored *in-utero* in these animals (13.0 ± 1.1 eggs) was comparable to wild-type animals (15.7 ±
358 1.2 eggs) and less than *egl-10(md176)* mutant animals (44.5 ± 2.3 eggs). These results
359 suggest that $G\alpha_o$ signals to inhibit HSN activity in a distinct manner from simple titration or
360 release of $\beta\gamma$ subunits.

361

362 **Egg-laying behavior is dysregulated in cAMP and cGMP signaling mutants**

363 $G\alpha_o$ is in the $G\alpha_{i/o}$ class of G proteins that bind to and inhibit nucleotide cyclases, which
364 function to reduce cAMP and cGMP levels and their subsequent activation of protein kinases
365 (Kobayashi et al., 1990; Zhang and Pratt, 1996; Matsubara, 2002; Ghil et al., 2006). The
366 hyperactive egg-laying behavior phenotypes of animals with reduced $G\alpha_o$ function could be
367 explained by a failure to properly terminate cAMP and/or cGMP signaling (Figure 5D, top). To
368 test this, we analyzed egg-laying behavior in strains bearing mutations that increase $G\alpha_s$ and
369 cAMP effector signaling (Reynolds et al., 2005; Schade et al., 2005; Charlie et al., 2006a; Charlie
370 et al., 2006b). Animals carrying *gsa-1(ce81)* gain-of-function mutations in $G\alpha_s$ predicted to
371 increase signaling accumulate fewer eggs compared to wild-type animals (Figure 5D, middle).
372 Because a reduction in steady-state egg accumulation could be caused by indirect effects of
373 these mutations on egg production or brood size, we also examined the developmental age of
374 embryos laid. As previously reported (Bany et al., 2003), loss of inhibitory $G\alpha_o$ signaling causes
375 embryos to be laid precociously, before they reach the 8-cell stage (Figure 5D, bottom). $G\alpha_s$
376 gain-of-function mutant animals do not show a corresponding increase in early-stage embryos
377 that are laid, suggesting the reduction in egg accumulation observed in $G\alpha_s$ gain-of-function
378 mutant animals is indirect. In contrast, gain-of-function *acy-1* Adenylate Cyclase mutations or

379 loss-of-function *pde-4* phosphodiesterase mutations, both predicted to result in increased
380 cAMP signaling, cause animals to accumulate fewer eggs and lay them at earlier stages
381 (Figure 5D). Similarly, *kin-2* mutations that disrupt an inhibitory regulatory subunit of Protein
382 Kinase A showed a modest but significant hyperactive egg-laying phenotype. Together, these
383 results indicate that $G\alpha_s$, cAMP, and Protein Kinase A signaling promote egg-laying behavior.
384 Because these mutant phenotypes were not nearly as strong as animals carrying $G\alpha_o$ mutants,
385 $G\alpha_o$ likely signals to inhibit egg laying via other effectors.

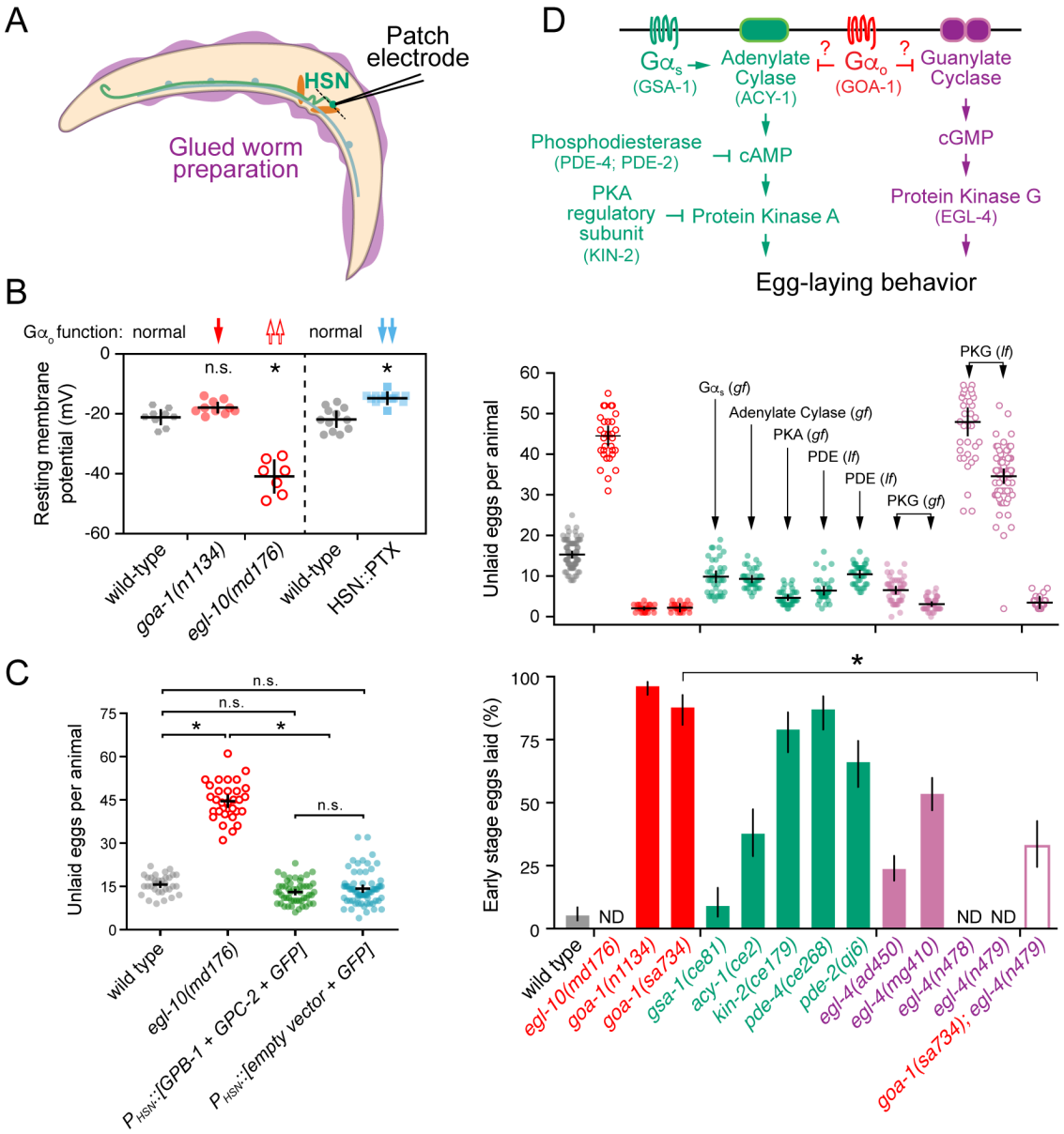

386

387 **Figure 5. Gα_o depresses HSN resting membrane potential and may inhibit egg-laying**
388 **behavior in parallel to $\beta\gamma$, cGMP, and cAMP signaling pathways.**

389 (**A**) Cartoon of the glued worm preparation used for patch clamp electrophysiology of HSN. (**B**)
390 Scatter plots show resting membrane potential of wild-type control animals (grey circles), *goa-*
391 *1(n1134)* loss-of-function mutants (red filled circles), *egl-10(md176)* null mutants (red open
392 circles), and in transgenic animals expressing Pertussis Toxin in HSN (blue filled squares).
393 Error bars indicate 95% confidence intervals for the mean. Asterisks indicate $p<0.0001$ (One-
394 Way ANOVA with Bonferroni correction for multiple comparisons). N≥7 animals recorded per
395 genotype. (**C**) Scatter plots show average number of eggs retained by wild-type animals (gray
396 filled circles), *egl-10(md176)* null mutants (orange open circles), and in transgenic animals
397 expressing either Gβ (GPB-2) and Gγ (GPC-1) subunits (green filled circles) or nothing (blue
398 filled circles) in HSN from the *tph-1* gene promoter along with GFP. Error bars indicate means
399 with 95% confidence intervals. Asterisk indicates $p<0.0001$; n.s. indicates $p>0.05$ (One-Way
400 ANOVA with Bonferroni correction for multiple corrections). (**D**) Top, cartoon of how Gα_o
401 signaling might interact with cAMP and cGMP signaling pathways. Gene names for *C. elegans*
402 orthologs tested here are indicated in parentheses. Middle, scatterplots show average number
403 of eggs retained by wildtype (grey), *egl-10(md176)* (red open circles), *goa-1(n1134)* and *goa-*
404 *1(sa734)* Gα_o loss of function (red filled circles) mutants, and in animals with altered cAMP
405 effector signaling (green): *gsa-1(ce81)* Gα_s gain-of-function, *acy-1(ce2)* Adenylate Cyclase
406 gain-of-function, *kin-2(ce179)* Protein Kinase A (PKA) inhibitory regulatory subunit loss-of-
407 function, *pde-4(ce268)* Phosphodiesterase (PDE) loss-of-function, *pde-2(qj6)*
408 Phosphodiesterase (PDE) null; altered cGMP effector signaling (pink): *egl-4(ad805)* and *egl-*
409 *4(mg410)* Protein Kinase G (PKG) gain-of-function (pink filled circles), *egl-4(n478)* and *egl-*
410 *4(n479)* loss-of-function mutants (pink open circles). Mean totals below ~10 eggs indicate
411 hyperactive egg laying while totals above ~20 eggs indicate egg-laying behavior defects.
412 Bottom, bar graphs indicate percent of embryos laid at early stages of development. Animals
413 laying ≥50% embryos at early stages are considered hyperactive. Error bars indicate ± 95%
414 confidence intervals for the mean proportion. N.D. indicates the stages of eggs laid was not
415 determined because those mutants are egg-laying defective (Egl). Asterisk indicates
416 highlighted significant differences ($p\leq0.0001$; Fisher Exact Test with Bonferroni correction for
417 multiple comparisons).

418

419 Extensive work has shown that the cGMP-dependent Protein Kinase G, EGL-4,
420 regulates egg laying in *C. elegans* (Fujiwara et al., 2002; L'Etoile et al., 2002; Raizen et al., 2006;
421 Hao et al., 2011). Mutations which increase EGL-4 activity cause hyperactive egg laying and
422 release of early stage embryos, while elimination of EGL-4 signaling causes egg-laying defects
423 and significant egg accumulation (Figure 5D, middle). To determine whether Gα_o and Protein
424 Kinase G regulate egg laying in a shared pathway, we performed a genetic epistasis
425 experiment. *goa-1(sa734)*; *egl-4(n479)* double null mutants accumulate very few eggs (Figure

426 5D, middle), resembling the *goa-1(sa734)* null mutant. However, the low brood size of the *goa-*
427 *1(sa734)* mutant could prevent accurate measurement of these animal's egg-laying defects. To
428 address this, we measured the stage of eggs laid as indicated above. Loss of the EGL-4
429 Protein Kinase G strongly and significantly suppressed the hyperactive egg-laying behavior of
430 $G\alpha_o$ null mutants (Figure 5D, bottom). *goa-1(sa734)*; *egl-4(n479)* mutants laid 33% of their
431 embryos at early stages compared to 88% for the *goa-1(sa734)* single mutant, an intermediate
432 egg-laying phenotype. These results are consistent with cGMP and/or Protein Kinase G
433 signaling acting downstream of $G\alpha_o$ in the proper regulation of egg-laying behavior.

434

435 **$G\alpha_o$ signals in the vulval muscles and uv1 neuroendocrine cells to inhibit egg laying**

436 In addition to HSN, GOA-1 is expressed in all neurons of the reproductive circuit, the
437 egg-laying vulval muscles, and the uv1 neuroendocrine cells (Mendel et al., 1995; Segalat et al.,
438 1995; Jose et al., 2007), raising questions as to how $G\alpha_o$ signaling functions in those other cells
439 to regulate egg-laying behavior. Previous work has shown that GOA-1(Q205L) was sufficient
440 to rescue the hyperactive egg-laying behavior of *goa-1(n1134)* mutants when expressed in the
441 HSNs but had little effect when expressed in the VCs or vulval muscles (Tanis et al., 2008).
442 Similarly, transgenic expression of Pertussis Toxin in the VCs or vulval muscles failed to
443 modify egg-laying behavior strongly (Tanis et al., 2008). Previous work failing to identify a
444 function for $G\alpha_o$ in the vulval muscles used a modified *Nde*-box element from the *ceh-24*
445 promoter that drives expression more efficiently in the vm1 muscle cells compared to the vm2
446 muscles innervated by the HSN and VC neurons (data not shown). We find that expression of
447 Pertussis Toxin in both vm1 and vm2 vulval muscles from a larger region of the *ceh-24* gene
448 promoter (Harfe and Fire, 1998; Ravi et al., 2018a) also failed to cause any significant changes

449 in the steady-state egg accumulation (Figure 6A). Conversely, expression of the activated
450 GOA-1(Q205L) mutant in the vulval muscles from the same promoter did cause a modest but
451 significant egg-laying defect, with animals accumulating 24.1 ± 2.0 eggs compared to
452 mCherry-expressing control transgenic animals (13.2±0.7 eggs). This egg-laying defect was
453 significantly weaker than *egl-10(md176)* mutants (46.0 ± 3.3 eggs) or transgenic animals
454 expressing GOA-1(Q205L) just in the HSNs (36.8 ± 3.8 eggs). We do not believe this modest
455 egg-laying defect was caused by transgene expression outside of the vulval muscles, as
456 blocking synaptic transmission via transgenic expression of Tetanus Toxin from the same *ceh-*
457 *24* promoter showed no such egg-laying defect (Figure 6B). Collectively, these results show
458 that $G\alpha_o$ does not play a significant role in suppressing vulval muscle excitability under state-
459 state conditions but that activated $G\alpha_o$ can signal in these cells to induce a mild but significant
460 inhibition of cell activity and egg-laying behavior.

461 The uv1 cells express the neurotransmitter tyramine along with NLP-7 and FLP-11
462 neuropeptides which inhibit egg laying (Alkema et al., 2005; Collins et al., 2016; Banerjee et al.,
463 2017). Based on the function of $G\alpha_o$ signaling in inhibiting neurotransmitter release in neurons,
464 we would expect that loss of $G\alpha_o$ function in uv1 would enhance their excitability, promoting
465 release of inhibitory tyramine and neuropeptides, causing a reduction of egg laying.
466 Surprisingly, previous work has shown that transgenic expression of Pertussis Toxin in uv1
467 cells increased the frequency of early-stage eggs that are laid, similar to the blocking of
468 neurotransmitter release by Tetanus Toxin (Jose et al., 2007). A caveat of these experiments is
469 that the *ocr-2* gene promoter used for transgene expression in uv1 also expresses in the utse
470 (uterine-seam) associated cells and head sensory neurons (Jose et al., 2007). To test whether
471 $G\alpha_o$ functions specifically in uv1 to regulate egg laying, we used the *tdc-1* gene promoter
472 (Alkema et al., 2005) along with the *ocr-2* 3' untranslated region (Jose et al., 2007) to drive

473 expression more specifically in uv1. Transgenic expression of Pertussis Toxin in uv1 caused a
474 mild but significant decrease in steady-state egg accumulation (10.9 ± 1.5 eggs) compared to
475 mCherry-expressing control animals (15.3 ± 1.2 eggs), indicating $G\alpha_o$ signaling facilitates uv1-
476 dependent inhibition of egg-laying behavior (Figure 6C). We also tested how increased $G\alpha_o$
477 signaling in uv1 affects egg laying. Transgenic expression of the activated GOA-1(Q205L)
478 mutant in uv1 cells caused no quantitative differences in egg accumulation (15.5 ± 2.1 eggs)
479 (Figure 6C). Together, these results show that $G\alpha_o$ has a limited role in regulating egg-laying
480 behavior in the vulval muscles or uv1 neuroendocrine cells, unlike the strong phenotypes
481 observed when we genetically manipulate $G\alpha_o$ function in HSN.

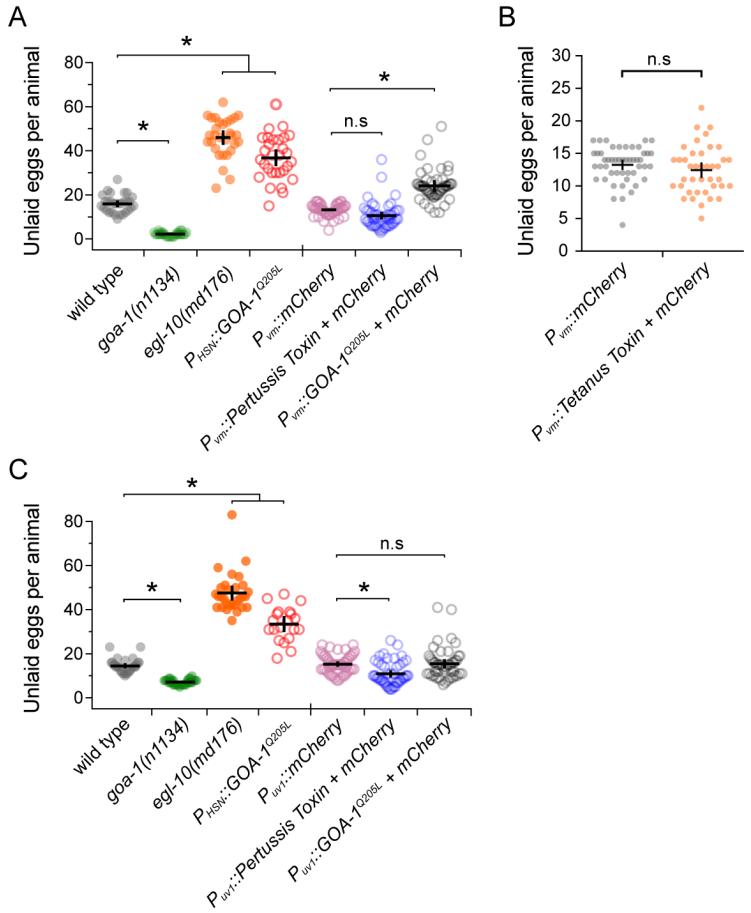

482

483 **Figure 6. Altered $G\alpha_o$ signaling in the vulval muscles and uv1 neuroendocrine cells**
484 **causes only modest effects on egg laying.**

485 **(A)** Scatter plots show average number of eggs retained by wild-type (grey), *goa-1(n1134)*
486 mutants (green), *egl-10(md176)* null mutant animals (orange) along with transgenic animals
487 expressing GOA-1^{Q205L} in the HSNs (red open circles) compared to transgenic animals
488 expressing mCherry only (pink open circles), Pertussis Toxin (blue open circles), or GOA-
489 1^{Q205L} (black open circles) in the vulval muscles from the *ceh-24* gene promoter. (**B**) Scatter
490 plots show average number of eggs retained in transgenic animals expressing mCherry only
491 (gray) or Tetanus Toxin along with mCherry (orange) in the vulval muscles (vm) using the *ceh-*
492 *24* gene promoter. Error bars indicate means with 95% confidence intervals. (**C**) Scatter plots
493 show average number of eggs retained by wild-type (grey), *goa-1(n1134)* mutant (green), *egl-*
494 *10(md176)* null mutant (orange) animals, and transgenic animals expressing GOA-1^{Q205L} in the
495 HSNs (red) compared to transgenic animals expressing mCherry only (pink), Pertussis Toxin
496 (blue), or GOA-1^{Q205L} (black open circles) in the uv1 neuroendocrine cells from the *tdc-1* gene
497 promoter. Four or five independent extrachromosomal arrays were generated for each
498 transgene in **(A-C)** and ~10 animals bearing each extrachromosomal array were analyzed.
499 Error bars indicate 95% confidence intervals for the mean. Asterisks indicate $p<0.0001$; n.s.
500 indicates $p>0.05$ (One-Way ANOVA with Bonferroni's correction for multiple comparisons or
501 Student's t test).

502

503 **NLP-7 inhibition of HSN activity and egg-laying requires the EGL-47 receptor and Gα_o**

504 Multiple neuropeptides and receptors have been identified to inhibit egg laying by
505 signaling through Gα_o-coupled receptors expressed on HSN (Figure 1A). Recent work has
506 identified NLP-7 neuropeptides, synthesized in the VC neurons and uv1 neuroendocrine cells,
507 as potential ligands for EGL-47 receptor signaling through Gα_o (Moresco and Koelle, 2004;
508 Banerjee et al., 2017). Animals overexpressing the NLP-7 neuropeptide are egg-laying
509 defective, accumulating 39.6 ± 3.4 eggs in the uterus (Figure 7A). To test how NLP-7 inhibits
510 egg laying, we crossed NLP-7 over-expressing transgenes into *goa-1* mutant animals and
511 evaluated their egg-laying behavior phenotypes. As shown in Figure 7A, the hypomorphic *goa-*
512 *1(n1134)* loss-of-function mutant significantly suppressed these egg-laying defects, as
513 previously shown (Banerjee et al., 2017). However, the suppression by *goa-1(n1134)* was
514 incomplete; NLP-7 over-expressing, *goa-1(n1334)* double mutant animals retained more eggs
515 than the *goa-1(n1134)* single mutant or even wild-type control animals (Figure 7A). To confirm
516 whether Gα_o was required for NLP-7 inhibition, we tested the *goa-1(sa734)* null mutant and

517 found it fully suppressed the egg-laying defects caused by NLP-7 over-expression. To confirm
518 this epistatic relationship, we measured the stage of embryos laid by these animals. *goa-*
519 *1(sa734)* null mutant animals over-expressing NLP-7 laid ~100% of their embryos at early
520 stages, a level not significantly different *goa-1(sa734)* single mutant animals (Figure 7B).
521 Together, these results show that NLP-7 neuropeptides cannot inhibit egg-laying behavior in
522 the absence of $G\alpha_o$ function.

523 Since the HSNs appear to be the principal sites of inhibitory $G\alpha_o$ signaling, we tested
524 how NLP-7 over-expression affects HSN Ca^{2+} activity. As expected, over-expression of NLP-7
525 strongly inhibited HSN Ca^{2+} activity (Figure 7C and 7D), consistent with the strong egg-laying
526 defects of these animals. To our surprise, loss of $G\alpha_o$ in these animals did now show high
527 frequency HSN Ca^{2+} transient activity, despite showing the strong hyperactive egg-laying
528 behavior of *goa-1(sa734)* single mutants (Figure 7C and 7D). This result shows that the
529 hyperactive egg-laying behavior of $G\alpha_o$ null mutants is unlinked to the increase in HSN Ca^{2+}
530 activity we observe. Previous work showed NLP-7 inhibition of HSN activity and egg laying
531 requires the EGL-47 receptor (Banerjee et al., 2017). To show directly whether NLP-7 inhibition
532 of HSN activity requires the EGL-47 receptor, we recorded HSN Ca^{2+} activity in *egl-47(ok677)*
533 null mutants. Unexpectedly, animals lacking EGL-47 had significantly fewer HSN Ca^{2+}
534 transients than wild-type animals whether or not NLP-7 was over-expressed (Figure 7D).
535 These results show that although NLP-7 signals to silence HSN Ca^{2+} activity, it does not
536 require EGL-47 or $G\alpha_o$ function to do so.

537

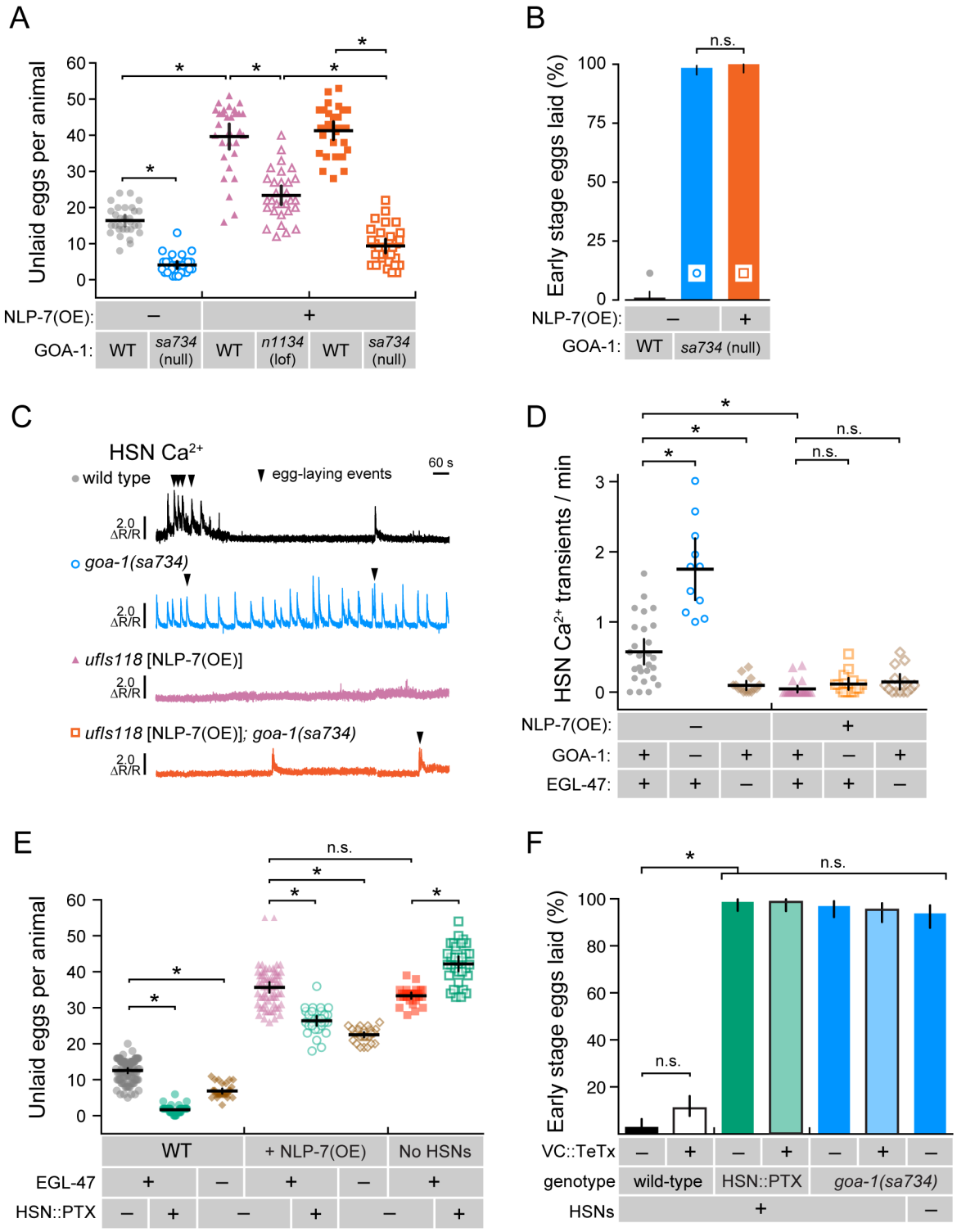

Figure 7. NLP-7 neuropeptides signal through EGL-47 and Gα$_o$ to inhibit egg-laying outside of the HSNs

(A) NLP-7 signals through Gα$_o$ to inhibit egg-laying behavior. Scatter plots show average number of eggs retained by wild-type (gray circles), *goa-1(sa734)* mutants (blue open circles), NLP-7 over-expressing (OE) transgenics in the wild-type (pink triangles or orange squares),

544 and in NLP-7 over-expressing transgenics in the *goa-1(n1134)* (pink open triangles) and *goa-*
545 *1(sa734)* null mutant background (orange open squares). Data in orange squares are from
546 animals that also carry the *vsIs183* transgene used for HSN Ca^{2+} imaging. Mean totals below
547 ~10 eggs indicate hyperactive egg laying while totals above ~20 eggs indicate egg-laying
548 defective behavior defects. Error bars indicate 95% confidence intervals for the mean.
549 Asterisks indicate $p<0.0001$ (One-Way ANOVA with Bonferroni correction for multiple
550 comparisons). N≥30 animals for each strain. (**B**) Measure of early stage eggs laid by wild-type
551 (black), *goa-1(sa734)* null mutants (blue), and *goa-1(sa734)* null mutants over-expressing
552 NLP-7 neuropeptides (orange). Both *goa-1(sa734)* mutant strains also carry the *vsIs183*
553 transgene used for HSN Ca^{2+} imaging. (**C**) NLP-7 over-expression silences HSN Ca^{2+} activity.
554 Representative GCaMP5/mCherry ratio traces showing HSN Ca^{2+} activity in wild-type (black),
555 *goa-1(sa734)* null mutants, and NLP-7 overexpressing transgenic animals in the wild-type
556 (pink) and *goa-1(sa734)* null mutant backgrounds (orange). Arrowheads indicate egg-laying
557 events. **(D)** Scatter plots show HSN Ca^{2+} peaks per minute measurements in wild-type (black),
558 *goa-1(sa734)* null mutants, or *egl-47(ok677)* null mutant animals in the absence or presence of
559 NLP-7 over-expression (OE). Error bars indicate 95% confidence intervals for the mean for
560 N≥10 animals; n.s. indicates $p>0.05$ while asterisk indicates $p\leq0.0001$ (one-way ANOVA with
561 Bonferroni correction for multiple comparisons). **(E)** NLP-7 inhibition of egg laying is not
562 exclusive to HSN silencing. Scatter plots show the average number of eggs retained by wild-
563 type animals, transgenic animals expressing Pertussis Toxin in HSN, and *egl-47(ok677)*
564 mutant animals in the absence or presence of NLP-7 over-expression (OE) or the absence of
565 HSNs. Error bars indicate 95% confidence intervals for the mean. Asterisks indicate $p<0.0001$
566 (One-Way ANOVA with Bonferroni correction for multiple comparisons); N≥30 animals for each
567 strain. (**F**) Measure of early stage eggs laid by wild-type or transgenic animals expressing
568 Tetanus Toxin the VC neurons (black outlined boxes) in animals expressing Pertussis Toxin in
569 the HSNs (green) or in *goa-1(sa734)* animals missing $G\alpha_o$ (blue). Error bars indicate ± 95%
570 confidence intervals for the mean proportion. Asterisk indicates highlighted significant
571 differences ($p\leq0.0001$) while n.s. indicates $p>0.05$ (Fisher Exact Test with Bonferroni
572 correction for multiple comparisons).

573

574 To confirm whether NLP-7 inhibition of egg laying requires EGL-47 and $G\alpha_o$ function
575 outside of HSN, we compared egg-laying behavior in NLP-7 transgenic animals where $G\alpha_o$
576 and synaptic transmission were blocked in defined cells of the egg-laying circuit. As expected
577 from our Ca^{2+} imaging experiments, NLP-7 over-expressing animals accumulated a similar
578 number of eggs as *egl-1(n986dm)* animals lacking HSNs (35.7 ± 1.4 eggs vs. 33.4 ±0.9 eggs
579 Figure 7E). Transgenic expression of Pertussis Toxin in HSNs or loss of the EGL-47 receptor
580 weakly suppressed egg accumulation in NLP-7 over-expressing animals (Figure 7E). The
581 suppression of NLP-7 egg-laying defects by Pertussis Toxin expression was specific, as *egl-*

582 *1(n986dm)* animals developmentally lacking HSNs showed no comparable decrease in egg
583 retention and showed a mild but significant increase (Figure 7E), possibly through co-
584 expression of Pertussis Toxin from the transgene in the NSMs (Tanis et al., 2008). Thus, NLP-7
585 inhibits egg laying, in part, through an inhibitory G protein like $G\alpha_o$ in HSN and the EGL-47
586 receptor. Because whole-animal, but not HSN-specific, elimination of $G\alpha_o$ function completely
587 suppressed NLP-7-induced egg-laying defects (Figure 7A), these data show that NLP-7
588 signals to inhibit egg laying through $G\alpha_o$-coupled receptors on cells other than HSN. The
589 cholinergic VC neurons also make extensive synapses onto the vulval muscles, suggesting
590 they may act alongside the HSNs to promote vulval muscle contractility and egg laying (White
591 et al., 1986; Waggoner et al., 1998). To test whether enhanced VC neurotransmitter release was
592 driving the hyperactive egg-laying behavior of $G\alpha_o$ signaling mutants, we transgenically
593 expressed Tetanus Toxin in the VC neurons using a cell-specific promoter (Bany et al., 2003).
594 Loss of VC synaptic transmission had no effect on egg-laying behavior by *goa-1(sa734)* null
595 mutants or animals expressing Pertussis Toxin in HSN (Figure 7F). As previously reported
596 (Mendel et al., 1995; Segalat et al., 1995), we find that loss of $G\alpha_o$ also bypasses the regulation
597 by of egg laying by the HSNs, as *goa-1(sa734)*; *egl-1(n986dm)* double mutants
598 developmentally missing the HSNs still lay their eggs at early stages of development (Figure
599 7F). Together, these results show that NLP-7 neuropeptides and $G\alpha_o$ signal to inhibit egg-
600 laying behavior through cellular targets other than the VCs and HSNs.

601

602

603 **Discussion**

604 Using a combination of genetic, imaging, physiological, and behavioral approaches, we
605 found that the conserved G protein, $G\alpha_o$, signals to depress activity in the *C. elegans* egg-
606 laying circuit, preventing entry into the active behavior state. Neuropeptides, released in
607 response to aversive external sensory input and feedback of successful egg release, activate
608 inhibitory receptors and $G\alpha_o$ which signal to reduce cell electrical excitability and
609 neurotransmitter release. Without inhibitory $G\alpha_o$ signaling, the presynaptic HSN command
610 neurons remain electrically excited, rendering them resistant to inhibitory sensory input and
611 feedback from the stretch-dependent homeostat. As a result, animals lacking $G\alpha_o$ enter the
612 egg-laying active state twice as frequently as wild-type animals and in environments that would
613 normally be unfavorable for egg laying. Thus, inhibitory $G\alpha_o$ signaling allows for a two-state
614 pattern of circuit activity that can be properly gated by external and internal sensory input.

615 Our results inform our understanding of how G protein signaling modulates the stretch-
616 dependent homeostat that governs egg-laying behavior. Even in 'optimal' environmental
617 conditions including abundant food, egg laying in wild-type animals typically begins ~6 hours
618 after the L4-adult molt upon the accumulation of 5-8 eggs in the uterus (Ravi et al., 2018a). Loss
619 of inhibitory $G\alpha_o$ signaling causes precocious egg laying, with eggs being released soon after
620 being deposited into the uterus. Animals lacking $G\alpha_o$ function in HSN show tonic Ca^{2+} transient
621 activity even after chemical sterilization, conditions that normally inhibit HSN and vulval muscle
622 Ca^{2+} activity in wild-type animals. Genetic perturbations that increase inhibitory $G\alpha_o$ signaling
623 delay egg laying until ~18 hours after the molt, like animals lacking HSNs altogether. Egg
624 laying in animals with reduced or eliminated HSN function resumes when the accumulation of
625 eggs activates the circuit via the stretch-dependent homeostat (Collins et al., 2016; Ravi et al.,

626 2018a). Wild-type animals acutely exposed to aversive sensory conditions show a rapid
627 inhibition of HSN activity and egg laying (Sawin, 1996; Zhang et al., 2008; Fenk and de Bono,
628 2015), but they continue to make and accumulate eggs in the uterus. Egg laying resumes upon
629 removal of the inhibitory sensory stimulus or a return to food (Sawin, 1996; Dong et al., 2000).
630 Feedback of egg accumulation and release has long-term consequences on female
631 reproductive physiology. The cGMP-dependent Protein Kinase G ortholog, EGL-4, regulates
632 the expression of a novel secreted protein in the uterine epithelium whose levels correlate with
633 egg-laying rate (Hao et al., 2011). Feedback of egg release regulates *tph-1* gene expression
634 that increases serotonin biosynthesis in the HSNs, alters sensory responses to male
635 pheromone, and germline precursor cell proliferation (Aprison and Ruvinsky, 2019b, a).
636 Because the primary function of all adult *C. elegans* behaviors is survival and reproduction, we
637 hypothesize that most or all salient sensory signals ultimately converge to modulate egg-laying
638 circuit activity and animal fecundity.

639 Our work shows that $G\alpha_o$ also signals in cells other than HSN to inhibit egg-laying circuit
640 activity and behavior. GOA-1 is likely expressed in all electrically excitable cells including all
641 cells in the egg-laying circuit (Mendel et al., 1995; Segalat et al., 1995; Jose et al., 2007). Over-
642 expression of NLP-7 neuropeptides strongly inhibits HSN Ca^{2+} activity and egg-laying
643 behavior. While complete loss of $G\alpha_o$ suppresses egg-laying defects caused by NLP-7
644 overexpression, HSN Ca^{2+} activity remains largely inhibited. This suggests NLP-7 signals
645 through $G\alpha_o$ to inhibit egg laying in cells other than HSN. Consistent with this result, *goa-1* null
646 mutants remain strongly hyperactive for egg laying even when HSN or VC synaptic
647 transmission is blocked. Where else does $G\alpha_o$ function to inhibit egg laying? While $G\alpha_o$ is
648 expressed in the vulval muscles, transgenic expression of Pertussis Toxin or a GTP-locked
649 form of $G\alpha_o$ causes only modest egg-laying defects. Extensive work has shown that $G\alpha_o$

650 signals to inhibit release of acetylcholine from motor neurons during locomotion (Miller et al.,
651 1999; Nurrish et al., 1999). EM reconstruction that revealed the *C. elegans* synaptic wiring
652 diagram shows that the VA7 and VB6 cholinergic motor neurons that drive body wall muscle
653 contraction for locomotion also synapse onto the vm1 vulval muscles (White et al., 1986).
654 Recent work employing a new fluorescent reporter of acetylcholine shows rhythmic activity in
655 the vm1 muscles (Borden et al., 2020), and this vm1 activity is precisely where we observe
656 weak vulval muscle 'twitch' Ca^{2+} transients (Collins et al., 2016; Brewer et al., 2019). Mutations
657 that increase $G\alpha_s$ and cAMP signaling increase acetylcholine release from motor neurons and
658 promote locomotion (Reynolds et al., 2005; Schade et al., 2005; Charlie et al., 2006a; Charlie et al.,
659 2006b), possibly explaining why these mutations also increase egg laying. We predict that
660 cholinergic neurons like VA7 and VB6, or their command interneurons, express neuropeptide
661 and neurotransmitter receptors that signal through $G\alpha_o$ to depress acetylcholine release and
662 excitation of the vulval muscles. Identifying where such receptors are expressed and how they
663 signal will help explain how each cell in the circuit functions to drive discrete steps in egg
664 laying (Brewer et al., 2019; Fernandez et al., 2020).

665 Our work supports a model where $G\alpha_o$ inhibits synaptic transmission via modulation of
666 presynaptic ion channels. Genetic studies in *C. elegans* have identified the IRK inward
667 rectifying K^+ channels, NCA Na^+ leak channels, and CCA-1 T-type voltage-gated Ca^{2+}
668 channels as potential targets of $G\alpha_o$ signaling (Yeh et al., 2008; Emtage et al., 2012; Topalidou et
669 al., 2017a; Zang et al., 2017). Inward rectifying GIRK K^+ channels are activated by release of $\beta\gamma$
670 subunits (Hille, 1994). Previous work has shown the IRK-1 K^+ channel is expressed in HSN
671 and is required for inhibition of egg laying by the $G\alpha_o$-coupled EGL-6 neuropeptide receptor
672 (Emtage et al., 2012). The egg-laying phenotypes of *irk-1* mutant animals are not as strong as
673 *goa-1* mutants, and over-expression of $\beta\gamma$ subunits in HSN causes little or no effect on egg

674 laying. These results suggest $G\alpha_o$ signals to inhibit HSN neurotransmitter release via
675 additional mechanism(s). NALCN Na^+ leak channels are also expressed in HSN, and gain-of-
676 function mutations increase HSN Ca^{2+} activity and drive hyperactive egg-laying and locomotion
677 behaviors (Yeh et al., 2008). NALCN channels are genetically downstream of both $G\alpha_q$ and $G\alpha_o$
678 in the regulation of dopamine signaling and locomotion, suggesting that NALCN channels
679 could be direct targets for modulation (Lutas et al., 2016; Topalidou et al., 2017b). Physiological
680 experiments in mammalian neurons support this model. NALCN currents are activated by
681 neuropeptide signaling through $G\alpha_q$ (Lu et al., 2009) and inhibited by dopamine and GABA
682 signaling through $G\alpha_{i/o}$ (Philippart and Khaliq, 2018). However, *C. elegans* knockout mutants in
683 NALCN channel components do not show the strong behavior defects seen in $G\alpha_q$ and $G\alpha_o$
684 mutants, suggesting other channels act in parallel to NALCN to regulate HSN and circuit
685 excitability. One candidate are TMC channels that drive a background Na^+ leak conductance
686 that promotes HSN and vulval muscle cell electrical excitability (Yue et al., 2018). TMC
687 channels may also regulate cell electrical excitability as mechanosensors (Pan et al., 2018;
688 Tang et al., 2020). Cl^- channels and transporter proteins also regulate HSN activity and egg-
689 laying behavior. CLH-3 is a swelling and hyperpolarization-activated, inwardly rectifying
690 chloride channel that inhibits HSN activity (Branicky et al., 2014). Dynamic expression of Cl^-
691 transporter proteins in the HSNs as animals mature into egg-laying adults regulates the Cl^-
692 reversal potential (Tanis et al., 2009; Bellemer et al., 2011; Han et al., 2015). Loss of KCC-2 or
693 ABTS-1 transporters flips the reduced egg laying behavior of *egl-47(dm)* mutants into
694 hyperactive egg laying. Modulation of Cl^- transporter expression or activity by G protein
695 signaling could drive the shifts in cell excitability we observe between the inactive and active
696 egg-laying behavior states.

697 The modulation of antagonistic cation and anion channels likely determines the Ca^{2+}
698 dependent spiking probability of cells in the egg-laying circuit. HSN expresses L-type, P/Q-
699 type, and T-type voltage-gated Ca^{2+} channels (Mathews et al., 2003; Zang et al., 2017), and
700 each contributes to a normal serotonin response and egg-laying behavior (Schafer and Kenyon,
701 1995; Lee et al., 1997; Kwok et al., 2006). The modest but significant changes in HSN resting
702 membrane potential we observe in $G\alpha_o$ signaling mutants are expected to alter the probability
703 of eliciting Ca^{2+} spiking activity. Ca^{2+}-dependent action potentials have been found in *C.*
704 *elegans* neurons and muscles (Gao and Zhen, 2011; Liu et al., 2011; Liu et al., 2018) and is
705 regulated by both L-type and T-type Ca^{2+} channels. T-type channels like CCA-1 can contribute
706 to a 'window current' where the channel can pass current at depolarized potentials that are
707 insufficient to trigger channel inactivation (Williams et al., 1997; Crunelli et al., 2005; Zang et al.,
708 2017). Activation of these window currents might allow neurons like HSN to shift from
709 spontaneous tonic firing to high frequency Ca^{2+} bursting. Future work leveraging the powerful
710 molecular tools uniquely available in *C. elegans* and the egg-laying circuit along with direct
711 physiological measurements of membrane potential will allow mechanistic insight into how
712 neuromodulators like serotonin and neuropeptides signal through effectors to shape patterns
713 of circuit activity that underlie distinct behavior states.

714

715

716 **Materials and Methods**

717 **Nematode Culture and Developmental Staging**

718 *Caenorhabditis elegans* hermaphrodites were maintained at 20°C on Nematode Growth
719 Medium (NGM) agar plates with *E. coli* OP50 as a source of food as described (Brenner,
720 1974). For assays involving young adults, animals were age-matched based on the timing of
721 completion of the L4 larval molt. All assays involving adult animals were performed using age-
722 matched adult hermaphrodites 20-40 hours past the late L4 stage. Table 2 lists all strains used
723 in this study and their genotypes.

724

725 **Plasmid and Strain Construction**

726 Calcium reporter transgenes

727 ***HSN Ca^{2+}:*** HSN Ca^{2+} activity was visualized using LX2004 *vsIs183* [*nlp-3::GCaMP5::nlp-3*
728 *3'UTR + nlp-3::mCherry::nlp-3 3'UTR + lin-15(+)*] *lite-1(ce314) lin-15(n765ts) X* strain
729 expressing GCaMP5G and mCherry from the *nlp-3* promoter as previously described (Collins
730 et al., 2016). To visualize HSN Ca^{2+} activity in $G\alpha_o$ signaling mutants, we crossed LX2004
731 *vsIs183 lite-1(ce314) lin-15(n765ts) X* males with MT2426 *goa-1(n1134) I*, DG1856 *goa-*
732 *1(sa734) I*, or MT8504 *egl-10(md176) V* hermaphrodites, and the fluorescent cross-progeny
733 were allowed to self, generating MIA210 *goa-1(n1143) I*; *vsIs183 X lite-1(ce314) lin-15*
734 *(n765ts) X,* MIA263 *goa-1(sa734) I*; *vsIs183 X lite-1(ce314) lin-15 (n765ts) X*, and MIA216 *egl-*
735 *10(md176) V; vsIs183 lite-1(ce314) lin-15(n765ts) X* strains, respectively. To visualize how
736 NLP-7 signals to inhibit HSN Ca^{2+} activity and egg laying, we crossed IZ1236 *ufIs118*
737 hermaphrodites (Banerjee et al., 2017) with LX2004 males. The fluorescent cross-progeny were
738 selfed, generating MIA293 *ufIs118; vsIs183 lite-1(ce314) lin-15(n765ts) X.* To test the

739 requirement for $G\alpha_o$ signaling in NLP-7 inhibition, we crossed N2 males into MIA263
740 hermaphrodites, and the *goa-1(sa734)*/+ I; *vsIs183 lite-1(ce314) lin-15 (n765ts) X*
741 heterozygous males obtained were then crossed with MIA293 hermaphrodites to generate
742 MIA294 *ufIs118; goa-1(sa734) I; vsIs183 lite-1(ce314) lin-15(n765ts) X*. In order to test
743 whether EGL-47 was a potential receptor for NLP-7, we crossed LX2004 males into RB850
744 *egl-47(ok677) V* hermaphrodites. The fluorescent cross-progeny were allowed to self and
745 homozygous *egl-47(ok677)* mutant animals were identified by duplex PCR genotyping with the
746 following oligos: CGTCACTTTTCCGTTGCTCTCTCATG,
747 GTAGCGGGAAAGATGGCAAGAAGTCG, and TCGGTGAAACTCATTGTGCTCATTGTGC,
748 creating MIA359 *egl-47(ok677) V; vsIs183 lite-1(ce314) lin-15(n765ts) X.* Wild-type N2 males
749 were then crossed to MIA359 hermaphrodites, and the male *egl-47(ok677)/+ V; vsIs183 lite-*
750 *1(ce314) lin15(n765ts) X* cross progeny were then crossed with MIA293 hermaphrodites. The
751 cross-progeny were selfed and genotyped for the *egl-47(ok677) V* deletion mutant, generating
752 MIA366 *ufIs118; egl-47(ok677) V; vsIs183 lite-1(ce314) lin-15(n765ts) X.*

753 During the course of crossing the *vsIs50* transgene expressing the catalytic subunit of
754 Pertussis Toxin in the HSNs from the *tph-1* promoter (Tanis et al., 2008), we noticed repulsion
755 between *vsIs183*, suggesting both were linked to the X chromosome. As such, LX850 *vsIs50*
756 *lin-15(n765ts) X* males were crossed with LX1832 *lite-1(ce314) lin-15(n765ts) X*
757 hermaphrodites, the non-Muv progeny were selfed, and homozygous *lite-1(ce314)* non-Muv
758 animals were kept, generating the strain MIA218 *vsIs50 lite-1(ce314) lin-15(n765ts) X.* MIA218
759 males were then crossed with LX2007 *vsIs186; lite-1(ce314) lin-15(n765ts) X*; the cross-
760 progeny were selfed, generating MIA227 *vsIs186; vsIs50 lite-1(ce314) lin-15(n765ts) X*. To test
761 whether $G\alpha_o$ acts in HSN to mediate NLP-7 inhibition, we crossed wild-type N2 males into
762 LX2007 *vsIs186; lite-1(ce314) lin-15 (n765ts) X* hermaphrodites, and the heterozygous

763 *vsIs186*/+; *lite-1(ce314) lin-15 (n765ts) X* cross-progeny were mated with IZ1236 *ufIs118*
764 hermaphrodites. The fluorescent cross-progeny were selfed, creating MIA358 *ufIs118; vsIs186*
765 *lite-1(ce314) lin-15(n765ts) X*. Wild-type N2 males were then crossed into MIA227
766 hermaphrodites to generate heterozygous *vsIs186*/+*; vsIs50 lite-1(ce314) lin-15(n765ts) X*
767 males which were then crossed into MIA358 hermaphrodites. The fluorescent cross-progeny
768 were selfed, generating MIA360 *ufIs118; vsIs50; vsIs186; lite-1(ce314) lin-15(n765ts) X*.
769 Heterozygous *vsIs186*/+*; vsIs50 lite-1(ce314) lin-15(n765ts) X* males were also crossed into
770 MIA123 *egl-1(n986dm)* V; *lite-1(ce314) lin-15(n765ts)* X hermaphrodites, the fluorescent cross-
771 progeny were selfed, and Egl non-Muv animals were selected, generating MIA369 *egl-*
772 *1(n986dm) V; vsIs50; vsIs186 lite-1(ce314) lin-15 (n765ts) X*. The presence of the *egl-*
773 *1(n986dm)* allele was confirmed with snip-SNP PCR genotyping using oligonucleotides
774 CTCTGTTCCAGCTCAAATTTCC and GTAGTTGAGGATCTCGCTTCGGC followed by NciI
775 digestion.

776 In order to visualize HSN Ca^{2+} activity in transgenic animals expressing a constitutively active
777 mutant GOA-1^{Q205L} protein that increases $G\alpha_o$ signaling in the HSN neurons, LX2004 *vsIs183*
778 *lite-1(ce314) lin-15(n765ts) X* males were crossed with LX849 *vsIs49; lin-15(n765ts) X*
779 hermaphrodites. We noted a repulsion between *vsIs183* and *vsIs49* transgenes integrated on
780 X. As such, we selected a strain MIA277 with trans-heterozygous *vsIs49* and *vsIs183*
781 transgenes (*lite-1(ce314) vsIs49 X / lite-1(ce314) vsIs183 X*) for Ca^{2+} imaging. The MIA277
782 strain was maintained by picking phenotypically egg-laying defective adult animals which show
783 GCaMP5G/mCherry expression.

784 ***Vulval Muscle Ca^{2+}:*** Vulval muscle Ca^{2+} activity was recorded in adult animals using LX1918
785 *vsIs164* [*unc-103e::GCaMP5::unc-54 3'UTR + unc-103e::mCherry::unc-54 3'UTR + lin-15(+)*]
786 *lite-1(ce314) lin-15(n765ts) X* strain as described (Collins et al., 2016). To visualize vulval

787 muscle activity in $G\alpha_o$ signaling mutants, LX1918 males were crossed with MT2426 *goa-*
788 *1(n1134)* I and DG1856 *goa-1(sa734) I* hermaphrodites, and the fluorescent cross-progeny
789 were selfed, generating MIA214 *goa-1(n1134) I; vsIs164 lite-1(ce314) lin-15(n765ts) X* and
790 MIA295 *goa-1(sa734) I*; *vsIs164 lite-1(ce314) lin-15(n765ts) X* strains, respectively. To
791 visualize vulval muscle activity in transgenic animals expressing the catalytic subunit of
792 Pertussis Toxin in the HSN neurons (Tanis et al., 2008), MIA218 *vsIs50 lite-1(ce314) lin-*
793 *15(n765ts) X* males were crossed with LX1919 *vsIs165* [*unc-103e::GCaMP5::unc-54 3'UTR +*
794 *unc-103e::mCherry::unc-54 3'UTR + lin-15(+)*]*; lite-1(ce314) lin-15(n765ts) X* hermaphrodites,
795 and the cross progeny were selfed, generating MIA245 *vsIs50; vsIs165; lite-1(ce314) lin-*
796 *15(n765ts) X*. To visualize vulval muscle activity in transgenic animals expressing a
797 constitutively active mutant GOA-1^{Q205L} protein which increases $G\alpha_o$ signaling in the HSN
798 neurons (Tanis et al., 2008), LX849 *vsIs49; lin-15(n765ts) X* males were crossed with LX1919
799 *vsIs165; lite-1(ce314) lin-15(n765ts) X* hermaphrodites and the fluorescent cross-progeny were
800 selfed, generating MIA291 *vsIs165; vsIs50 lite-1(ce314) lin-15(n765ts) X*.
801
802 Transgenes used to manipulate $G\alpha_o$ signaling and synaptic transmission in specific cells of the
803 egg-laying circuit
804 ***HSN neurons***: To produce a HSN (and NSM)-specific GPB-1 expressing construct, the *gpb-1*
805 cDNA fragment was amplified from pDEST-*gpb-1* (Yamada et al., 2009) using the following
806 oligonucleotides: 5'- GAGGCTAGCGTAGAAAAAATGAGCGAACTTGACCAACTTCGA-3' and
807 5'-GCGGGTACCTCATTAATTCCAGATCTTGAGGAACGAG-3'. The ~1 kb DNA fragment was
808 digested with NheI/KpnI and ligated into pJT40A (Tanis et al., 2008) to generate pBR30. To
809 produce an HSN (and NSM)-specific GPC-2 expressing construct, the *gpc-2* cDNA fragment
810 was amplified from worm genomic DNA using the following forward and reverse
811 oligonucleotides: 5'-GAGGCTAGCGTAGAAAAAATGGATAAATCTGACATGCAACGA-3' and

812 5'-GCGGGTACCTTAGAGCATGCTGCACTTGCT-3'. The ~250 bp DNA fragment was
813 digested with NheI/KpnI and ligated into pJT40A to generate pBR31. To co-overexpress the βγ
814 G protein subunits in the HSN neurons, we injected pBR30 (50 ng/μl), pBR31 (50 ng/μl), and
815 pJM60 [*ptph-1*::GFP] (80 ng/μl) (Moresco and Koelle, 2004) into the LX1832 *lite-1(ce314) lin-*
816 *15(n765ts)* animals along with pLI5EK (50 ng/μl), generating five independent
817 extrachromosomal transgenic lines which were used for behavioral assays. One representative
818 transgenic strain, MIA278 [*keyEx52*; *lite-1(ce314) lin-15(n765ts)*], was kept. To generate a
819 control strain for comparison in the egg-laying assays, we injected pJM66 [*ptph-1*::empty] (100
820 ng/μl) (Tanis et al., 2008) and pJM60 (80 ng/μl) into the LX1832 *lite-1(ce314) lin-15(n765ts)*
821 animals along with pLI5EK (50 ng/μl) generating five independent extrachromosomal control
822 transgenes which were used for behavioral assays. One representative transgenic strain,
823 MIA279 [*keyEx53*; *lite-1(ce314) lin-15(n765ts)*], was kept. To test how loss of HSNs affected
824 the hyperactive egg-laying behavior of *goa-1(sa734)* null mutants, we mated wild-type N2
825 males into MIA26 *egl-1(n986dm) V* hermaphrodites, and the heterozygous *egl-1(n986dm)*/+
826 male cross-progeny were then crossed into DG1856 *goa-1(sa734)* I hermaphrodites. Their
827 cross-progeny were selfed, and the presence of the *egl-1(n986dm)* and *goa-1(sa734)* were
828 confirmed by genotyping, creating MIA345 *goa-1(sa734)* I; *egl-1(n986dm)* V.
829 ***Vulval muscles***: pJT40A *Ptph-1*::Pertussis Toxin (Tanis et al., 2008) was digested with
830 NheI/KpnI and ligated into pBR3 (*Pceh-24*::mCherry) to generate pBR20. pBR20 [*Pceh-*
831 *24*::Pertussis Toxin] (10 ng/μl) and pBR3 [*Pceh-24*::mCherry] (10 ng/μl) were injected into the
832 LX1832 *lite-1(ce314) lin-15(n765ts)* animals along with pLI5EK (50 ng/μl) to generate five
833 independent extrachromosomal transgenes which were used for behavioral assays. One
834 representative transgenic strain, MIA257 [*keyEx46*; *lite-1(ce314) lin-15(n765ts)*], was kept. To
835 produce vulval muscle-specific GOA-1(Q205L), the coding sequence of GOA-1(Q205L) was
836 recovered from pJM70C (Tanis et al., 2008) after digestion with NheI/SacI and ligated into

837 pKMC188 (*Punc-103e*::GFP; (Collins and Koelle, 2013)) generating pKMC268 (*Punc-*
838 *103e::goa-1(Q205L)*). However, because the *unc-103e* promoter also directs expression in
839 neurons that might indirectly regulate egg laying, GOA-1(Q205L) coding sequences were
840 removed from pKMC268 by digesting with NheI/NcoI and ligated into pBR3 to generate
841 pBR21. pBR21 [*Pceh-24*::GOA-1^{Q205L}] (10 ng/µl) and pBR3 [*Pceh-24*::mCherry] (10 ng/µl)
842 were injected into the LX1832 *lite-1(ce314) lin-15(n765ts)* animals along with pLI5EK (50 ng/µl)
843 to generate five independent extrachromosomal transgenes which were used for behavior
844 assays. One representative transgenic strain, MIA258 [*keyEx47*; *lite-1(ce314) lin-15(n765ts)*],
845 was kept. To generate control strains for comparison in egg-laying assays, pBR3 [*Pceh-*
846 *24*::mCherry] (20 ng/µl) was injected into the LX1832 *lite-1(ce314) lin-15(n765ts)* animals
847 along with pLI5EK (50 ng/µl) to generate five independent extrachromosomal transgenes
848 which were used for behavioral assays. One representative control transgenic strain, MIA256
849 [*keyEx45*; *lite-1(ce314) lin-15(n765ts)*], was kept. To produce a vulval muscle-specific Tetanus
850 Toxin transgene, Tetanus Toxin coding sequences were amplified from pAJ49 (*Pocr-*
851 *2*::Tetanus toxin) (Jose et al., 2007) using the following oligonucleotides: 5'-
852 GAGGCTAGCGTAGAAAAAATGCCGATCACCATCAACAACTTC-3' and 5'-
853 GCGCAGGCGGCCGCTCAAGCGGTACGGTTGTACAGGTT-3'. The DNA fragment was
854 digested with NheI/NotI and ligated into pBR6 to generate pBR27. To block any possible
855 neurotransmitter release from the vulval muscles, pBR27 (10 ng/µl) and pBR3 (10 ng/µl) was
856 injected into the LX1832 *lite-1(ce314) lin-15(n765ts)* animals along with pLI5EK (50 ng/µl) to
857 generate five independent extrachromosomal transgenes which were used for behavior
858 assays. One representative transgenic strain, MIA262 [*keyEx51*; *lite-1(ce314) lin-15(n765ts)*],
859 was kept.
860 ***uv1 neuroendocrine cells****:* To generate a uv1 cell-specific Pertussis toxin transgene, pBR20
861 (*Pceh-24*::Pertussis toxin) was digested with NheI/NcoI and the coding sequences of Pertussis

862 Toxin were then ligated into pAB5 (*Ptdc-1*::mCherry::*ocr-2* 3'UTR) to generate pBR25. pBR25
863 [*Ptdc-1*::Pertussis Toxin] (10 ng/µl) and pAB5 [*Ptdc-1*::mCherry] (5 ng/µl) were injected into
864 LX1832 *lite-1(ce314) lin-15(n765ts)* animals along with pLI5EK (50 ng/µl) to generate five
865 independent extrachromosomal transgenes which were used for behavioral assays. One
866 representative transgenic strain, MIA260 [*keyEx49*; *lite-1(ce314) lin-15(n765ts)*], was kept. To
867 generate a uv1 cell-specific GOA-1(Q205L) transgene, pKMC268 (*Punc-103e*::GOA-
868 1(Q205L)) was digested with NheI/NcoI and the coding sequences of GOA-1(Q205L) were
869 then ligated into pBR25 to generate pBR26. To increase $G\alpha_o$ signaling in uv1 cells, we injected
870 pBR26 [*Ptdc-1*::GOA-1^{Q205L}] (10 ng/µl) and pAB5 [*Ptdc-1*::mCherry] (5 ng/µl) into the LX1832
871 *lite-1(ce314) lin-15(n765ts)* animals along with pLI5EK (50 ng/µl) to generate five independent
872 extrachromosomal transgenes which were used for behavioral assays. One transgenic strain
873 MIA261 [*keyEx50*; *lite-1(ce314) lin-15(n765ts)*] was kept. To generate a control strain for
874 comparison in our egg-laying assays, pAB5 [*Ptdc-1*::mCherry] (15 ng/µl) was injected into the
875 LX1832 *lite-1(ce314) lin-15(n765ts)* animals along with pLI5EK (50 ng/µl) to generate five
876 independent extrachromosomal transgenes which were used for behavioral assays. One
877 representative transgenic strain, MIA259 [*keyEx48*; *lite-1(ce314) lin-15(n765ts)*], was kept.
878 ***VC neurons:*** A ~1.4 kB DNA fragment encoding Tetanus Toxin was excised from pAJ49 (Jose
879 et al., 2007) using AgeI/XhoI and ligated into a similarly digested pKMC145 *(Plin-11::GFP::unc-*
880 *54 3' UTR)* (Collins et al., 2016) to generate pKMC282 *(Plin-11::TeTx::unc-54 3' UTR)*.
881 pKMC282 (50 ng/µl) was injected along with pL15EK (50 ng/µl; (Clark et al., 1994) into LX1832
882 *lite-1(ce314) lin-15(n765ts)* X generating 4 independent transgenic lines of which one, MIA113
883 *keyEx32 [Plin-11::TeTx::unc-54 3'UTR + lin-15(+)],* was used for integration. *keyEx32* was
884 integrated with UV/TMP generating three independent integrants (*keyIs32*, *keyIs33*, and
885 *keyIs46*). Each transgenic line was backcrossed six times to LX1832 generating strains
886 MIA144, MIA145, and MIA146. The behavioral characterization of these VC-silenced animals

887 will be described elsewhere in more detail. To eliminate HSNs in these VC-silenced animals,
888 wild-type N2 males were crossed into MIA26 *egl-1(n986dm) V* hermaphrodites, and the
889 heterozygous *egl-1(n986dm)*/+ males were then crossed to MIA146 *keyIs46*; *lite-1(ce314) lin-*
890 *15(n765ts) X* hermaphrodites, and the cross-progeny were then selfed, generating the
891 homozygous strain MIA173 *keyIs46*; *egl-1(n986dm) V*; *lite-1(ce314) lin-15(n765ts) X*. To test
892 whether synaptic transmission from the VCs was required for the hyperactive egg-laying
893 behavior of $G\alpha_o$ signaling mutants, wild-type N2 males were crossed to MIA227 *vsIs186;*
894 *vsIs50 lite-1(ce314) lin-15(n765ts) X* hermaphrodites and the resulting heterozygous cross-
895 progeny were then crossed MIA144 hermaphrodites, allowed to self, generating MIA370
896 *vsIs186; keyIs33; vsIs50 lite-1(ce314) lin-15(n765ts) X.* To test how complete loss of GOA-1
897 affected egg laying in VC-silenced animals, we crossed wild-type N2 males into DG1856 *goa-*
898 *1(sa734)* I hermaphrodites, and the heterozygous *goa-1(sa734)*/+ cross-progeny were then
899 mated with MIA144 hermaphrodites. The cross-progeny were allowed to self, generating
900 MIA371 *goa-1(sa734) I; keyIs33; lite-1(ce314) lin-15(n765ts) X.* The presence of *goa-1(sa734)*
901 was confirmed by Sanger sequencing.

902

903 **Fluorescence Imaging**

904 ***Ratiometric Ca^{2+} Imaging:*** Ratiometric Ca^{2+} recordings were performed on freely behaving
905 animals mounted between a glass coverslip and chunk of NGM agar, as previously described
906 (Collins and Koelle, 2013; Li et al., 2013; Collins et al., 2016; Ravi et al., 2018b). Briefly, recordings
907 were collected on an inverted Leica TCS SP5 confocal microscope using the 8 kHz resonant
908 scanner at ~20 fps at 256x256 pixel resolution, 12-bit depth and ≥2X digital zoom using a 20x
909 Apochromat objective (0.7 NA) with the pinhole opened to ~20 µm. GCaMP5G and mCherry

910 fluorescence was excited using a 488 nm and 561 nm laser lines, respectively. Adult
911 recordings were performed 24 hours after the late L4 stage. After staging, animals were
912 allowed to adapt for ~30 min before imaging. During imaging, the stage and focus were
913 adjusted manually to keep the relevant cell/pre-synapse in view and in focus.

914 Ratiometric analysis (GCaMP5:mCherry) for all Ca^{2+} recordings was performed after
915 background subtraction using Volocity 6.3.1 as described (Ravi et al., 2018a). The egg-laying
916 active state was operationally defined as the period one minute prior to the first egg-laying
917 event and ending one minute after the last (in the case of a typical active phase where 3-4
918 eggs are laid in quick succession). However, in cases where two egg-laying events were apart
919 by >60 s, peaks were considered to be in separate active phases and any transients observed
920 between were considered to be from an inactive state. In animals where we observed no Ca^{2+}
921 peaks during the entire recording, the total duration of the recording was considered as one,
922 long, inter-transient interval. In animals where we observed a single Ca^{2+} transient, the
923 duration from the start of the recording to the time of the Ca^{2+} transient and the time from the
924 Ca^{2+} transient to the end of the recording were defined as inter-transient intervals. Animals
925 overexpressing NLP-7 become highly egg-laying defective, and the embryonic expression of
926 mCherry from the *nlp-3* promoter in accumulated eggs interfered with the standard image
927 segmentation protocol based on the mCherry channel. For these animals, unambiguous Ca^{2+}
928 transient-dependent changes in GCaMP5 fluorescence localized at the HSN cell body were
929 scored manually, and the frequency of such events were calculated as the number of observed
930 events per unit recording time, typically 10-20 minutes.

931 **Behavior Assays and Microscopy**

932 ***Animal sterilization:*** Animals were sterilized using Floxuridine (FUDR) as described (Mitchell
933 et al., 1979; Collins et al., 2016; Ravi et al., 2018a). Briefly, 100 µl of 10 mg/ml FUDR was applied

934 to OP50 seeded NGM plates. Late L4 animals were then staged onto the FUDR plates and the
935 treated adults were imaged ~24 hours later.
936 ***Egg laying assays:*** Unlaid eggs were quantitated as described (Chase et al., 2004). Staged
937 adults were obtained by picking late L4 animals and culturing them for 30-40 hr at 20°C. The
938 percentage of early-stage eggs laid were quantified as described (Koelle and Horvitz, 1996). 30
939 staged adults were placed on a thin lawn of OP50 bacteria on a nematode growth medium
940 (NGM) agar plate (Brenner, 1974) and allowed to lay eggs for 30 min. This was repeated with
941 new sets of staged animals until a total of at least 100 laid eggs were analyzed. Each egg was
942 examined under a Leica M165FC stereomicroscope and categorized into the following
943 categories: eggs which have 1 cell, 2 cell, 3-4 cell, 5-8 cell, and embryos with >8 cells. Eggs
944 with eight cells or fewer were classified as "early stage."
945 ***Long-term recording of egg-laying behavior:*** Egg-laying behavior was recorded at 4-5
946 frames per second from 24-hour adults after transfer to NGM plates seeded with a thin lawn of
947 OP50 bacterial food using a Leica M165FC stereomicroscope and camera (Grasshopper 3,
948 4.1 Megapixel, USB3 CMOS camera, Point Grey Research). N2 wild-type and hyperactive
949 egg-laying mutant strains (MT2426 and LX850) were recorded for 3 hours, and the egg-laying
950 defective strains MT8504 and LX849 were recorded for 8-10 hours. Average duration of active
951 and inactive states from these recordings were calculated as described (Waggoner et al., 1998;
952 Waggoner et al., 2000).

953

954 **Electrophysiology**

955 Electrophysiological recordings were carried out on an upright microscope (Olympus BX51WI)
956 coupled with an EPC-10 amplifier and Patchmaster software (HEKA), as previously described

957 (Yue et al., 2018; Zou et al., 2018). Briefly, day 2 adult worms were glued on the surface of
958 Sylgard-coated coverslips using the cyanoacrylate-based glue (Gluture Topical Tissue
959 Adhesive, Abbott Laboratories). A dorsolateral incision was made using a sharp glass pipette
960 to expose the cell bodies of HSN neurons for recording. The bath solution contained (in mM)
961 145 NaCl, 2.5 KCl, 5 $CaCl_2$, 1 $MgCl_2$, and 20 glucose (325–335 mOsm, pH adjusted to 7.3).
962 The pipette solution contained (in mM) 145 KCl, 5 $MgCl_2$, 5 EGTA, 0.25 $CaCl_2$, 10 HEPES, 10
963 glucose, 5 Na_2ATP and 0.5 NaGTP (315–325 mOsm, pH adjusted to 7.2). The resting
964 membrane potentials were tested with 0 pA holding under the Current Clamp model of whole-
965 cell patch. The high Cl^- content of the intracellular solution used may contribute to the relatively
966 depolarized membrane potentials we observed (Liu et al., 2018).

967

968 **Experimental Design and Statistical Analysis**

969 Sample sizes for behavioral assays followed previous studies (Chase et al., 2004; Collins and
970 Koelle, 2013; Collins et al., 2016). No explicit power analysis was performed before the study.
971 Statistical analysis was performed using Prism v.6-8 (GraphPad). Ca^{2+} transient peak
972 amplitudes and inter-transient intervals were pooled from multiple animals (typically ~10
973 animals per genotype/condition per experiment). No animals or data were excluded. Individual
974 *p* values are indicated in each Figure legend, and all tests were corrected for multiple
975 comparisons (Bonferroni for ANOVA and Fisher exact test; Dunn for Kruskal-Wallis).

976

977 **Disclosures / Conflict of Interests**

978 The authors declare no conflicts of interest.

979

980 **Acknowledgements**

981 This work was funded by grants from the NIH (R01-NS086932) and NSF (IOS-1844657) to
982 KMC. RJK 3rd was supported by a University of Miami Maytag Fellowship. We thank Yuichi Iino
983 for sharing plasmids. Strains used in this study have been provided to the *C. elegans* Genetics
984 Center, which is funded by NIH Office of Research Infrastructure Programs (P40 OD010440).
985 We thank Dr. Addys Bode Hernandez and Michael Scheetz for technical assistance. We thank
986 Drs. Qiang Liu, James Baker, Julia Dallman, Laura Bianchi, Brock Grill, Peter Larsson,
987 Stephen Roper, along with members of the Collins lab for helpful discussions and feedback on
988 the manuscript.

989

990 **Video 1.** GCaMP5:mCherry ratio recording of HSN Ca^{2+} activity in a control, wild-type adult
991 animal during an egg-laying active state. High Ca^{2+} is indicated in red while low calcium is in
992 blue. Head is at left, tail is at right.

993 **Video 2.** GCaMP5:mCherry ratio recording of HSN Ca^{2+} activity in a *goa-1(n1134)* mutant
994 adult animal during an egg-laying active state. High Ca^{2+} is indicated in red while low calcium
995 is in blue. Head is at left, tail is at right.

996 **Video 3.** GCaMP5:mCherry ratio recording of HSN Ca^{2+} activity in a *goa-1(sa734)* null mutant
997 adult animal during an egg-laying active state. High Ca^{2+} is indicated in red while low calcium
998 is in blue. Head is at right, tail is at left.

999 **Video 4.** GCaMP5:mCherry ratio recording of HSN Ca^{2+} activity in a transgenic adult animal
1000 expressing Pertussis Toxin in the HSNs from the *tph-1* gene promoter during an egg-laying
1001 active state. High Ca^{2+} is indicated in red while low calcium is in blue. Head is at top, tail is at
1002 bottom.

1003 **Video 5.** GCaMP5:mCherry ratio recording of vulval muscle Ca^{2+} activity in a control wild-type
1004 adult animal during an egg-laying active state. High Ca^{2+} is indicated in red while low calcium
1005 is in blue. Head is at right, tail is at top.

1006 **Video 6.** GCaMP5:mCherry ratio recording of vulval muscle Ca^{2+} activity in a *goa-1(n1134)*
1007 mutant adult animal during an egg-laying active state. High Ca^{2+} is indicated in red while low
1008 calcium is in blue. Head is at right, tail is at left.

1009 **Video 7.** GCaMP5:mCherry ratio recording of vulval muscle Ca^{2+} activity in a transgenic adult
1010 animal expressing Pertussis Toxin in the HSNs from the *tph-1* gene promoter during an egg-
1011 laying active state. High Ca^{2+} is indicated in red while low calcium is in blue. Head is at left, tail
1012 is at right.

1013 ***Table 2.*** *Strain names and genotypes for all animals used in this study (behavior assays and*

1014 *calcium imaging)*

1015

Strain	Feature	Genotype	Reference
N2	Bristol wild-type strain	wild type	(Brenner, 1974)
DA521	EGL-4 (Protein Kinase G) gain-of-function mutant. Hyperactive egg laying, sluggish locomotion	*egl-4(ad805) IV*	(Raizen et al., 2006)
DG1856	GOA-1 ($G\alpha_o$) null mutant, hyperactive egg laying	*goa-1(sa734) I*	(Robatzek and Thomas, 2000)
IZ1236	NLP-7 overexpression	*ufIs118*	(Banerjee et al., 2017)
KG421	GSA-1 ($G\alpha_s$) gain-of-function mutant. Hyperactive locomotion	*gsa-1(ce81) I*	(Schade et al., 2005)
KG518	ACY-1 (Adenylate Cyclase) gain-of-function mutant. Hyperactive locomotion	*acy-1(ce2) III*	(Schade et al., 2005)
KG532	KIN-2 (Protein Kinase A inhibitory regulatory subunit) loss-of-function mutant. Hypersensitive to stimuli	*kin-2(ce179) X*	(Schade et al., 2005)
KG744	PDE-4 (phosphodiesterase) loss-of-function mutant, Hyperactive locomotion	*pde-4(ce268) II*	(Charlie et al., 2006a)
LX849	HSN and NSM activated GOA-1(Q205L), egg laying defective	*vsIs49; lin-15(n765ts) X*	(Tanis et al., 2008)
LX850	HSN and NSM Pertussis Toxin, hyperactive egg laying	*vsIs50; lin-15(n765ts) X*	(Tanis et al., 2008)
LX1832	Strain for transgene production, blue-light insensitive, multi-vulva at 20°C in the absence of *lin-15(+)* rescue transgene.	*lite-1(ce314) lin-15(n765ts) X*	(Gurel et al., 2012)
LX1918	vulval muscle GCaMP5, mCherry	*vsIs164 lite-1(ce314) lin-15(n765ts) X*	(Collins et al., 2016)
LX1919	Vulval muscle GCaMP5, mCherry	*vsIs165; lite-1(ce314) lin-15(n765ts) X*	(Collins et al., 2016)
LX2004	HSN GCaMP5, mCherry	*vsIs183 lite-1(ce314) lin-15(n765ts) X*	(Collins et al., 2016)
LX2007	HSN GCaMP5, mCherry	*vsIs186 lite-1(ce314) lin-15(n765ts) X*	(Collins et al., 2016)
MIA26	no HSNs	*egl-1(n986dm) V*	(Garcia and Collins, 2019)
MIA36	EGL-4 (Protein Kinase G) gain-of-function mutant. Hyperactive egg laying, sluggish locomotion	*egl-4(mg410) IV*	(Hao et al., 2011)
MIA123	no HSNs with lin-15 marked transgenes	*egl-1(n986dm) V; lite-1(ce314) lin-15(n765ts) X*	this study

MIA144	VC Tetanus Toxin	*keyIs33; lite-1(ce314) lin-15(n765ts) X*	this study
MIA210	GOA-1 ($G\alpha_o$) reduced-function mutant; HSN GCaMP, mCherry	*goa-1(n1134) I; vsIs183 lite-1(ce314) lin-15(n765ts) X*	this study
MIA214	GOA-1 ($G\alpha_o$) reduced-function mutant; vulval muscle GCaMP5, mCherry	*goa-1(n1134) I; vsIs164 lite-1(ce314) lin-15(n765ts) X*	this study
MIA216	Increased $G\alpha_o$ signaling; HSN GCaMP5, mCherry	*egl-10(md176) V; vsIs183 lite-1(ce314) lin-15(n765ts) X*	this study
MIA218	HSN and NSM Pertussis Toxin in blue-light insensitive, *lin-15* multi-vulva background	*vsIs50 lite-1(ce314) lin-15(n765ts) X*	this study
MIA227	HSN and NSM Pertussis Toxin; HSN GCaMP5, mCherry	*vsIs186; vsIs50 lite-1(ce314) lin-15(n765ts) X*	this study
MIA245	HSN and NSM Pertussis Toxin; vulval muscle GCaMP5, mCherry	*vsIs50 X vsIs165; lite-1(ce314) lin-15(n765ts) X*	this study
MIA256	Vulval muscle mCherry (*ceh-24* promoter)	*keyEx45; lite-1(ce314) lin-15(n765ts) X*	this study
MIA257	Vulval muscle mCherry + Pertussis Toxin (*ceh-24* promoter)	*keyEx46; lite-1(ce314) lin-15(n765ts) X*	this study
MIA258	Vulval muscle mCherry + Activated GOA-1(Q205L) (*ceh-24* promoter)	*keyEx47; lite-1(ce314) lin-15(n765ts) X*	this study
MIA259	uv1 cells mCherry (*tdc-1* promoter, *ocr-2* 3' UTR)	*keyEx48; lite-1(ce314) lin-15(n765ts) X*	this study
MIA260	uv1 cells mCherry + Pertussis Toxin (*tdc-1* promoter, *ocr-2* 3' UTR)	*keyEx49; lite-1(ce314) lin-15(n765ts) X*	this study
MIA261	uv1 cells mCherry + Activated GOA-1(Q205L) (*tdc-1* promoter, *ocr-2* 3' UTR)	*keyEx50; lite-1(ce314) lin-15(n765ts) X*	this study
MIA262	Vulval muscle mCherry + Tetanus toxin (*ceh-24* promoter)	*keyEx51*; *lite-1(ce314) lin-15(n765ts) X*	this study
MIA263	GOA-1 ($G\alpha_o$) null mutant; HSN GCaMP5, mCherry	*goa-1(sa734) I; vsIs183 lite-1(ce314) lin-15(n765ts) X*	this study
MIA277	Increased $G\alpha_o$ signaling in HSN; HSN GCaMP5, mCherry	*vsIs49/+, +/vsIs183 lite-1(ce314) lin-15(n765ts) X (trans-heterozygote)*	this study
MIA278	HSN/NSM *gpb-1* and *gpc-2* overexpression + GFP (*tph-1* promoter)	*keyEx52; lite-1(ce314) lin-15(n765ts) X*	this study
MIA279	HSN/NSM empty + GFP (*tph-1* promoter)	*keyEx53; lite-1(ce314) lin-15(n765ts) X*	this study
MIA282	PDE-2 (phosphodiesterase) loss-of-function mutant	*pde-2(qj6)*	(Fujiwara et al., 2015)

MIA291	Increased $G\alpha_o$ signaling in HSN; vulval muscle GCaMP5, mCherry	*vsIs49; vsIs165 lite-1(ce314) lin-15(n765ts) X*	this study
MIA293	NLP-7 overexpression; HSN GCaMP5, mCherry	*ufIs118; vsIs183 lite-1(ce314) lin-15(n765ts) X*	(Banerjee et al., 2017) & this study
MIA294	NLP-7 overexpression; *goa-1(Gα$_o$)* null mutant; HSN GCaMP5, mCherry	*ufIs118; goa-1(sa734) I; vsIs183 lite-1(ce314) lin-15(n765ts) X*	(Banerjee et al., 2017) & this study
MIA295	GOA-1 ($G\alpha_o$) mutant, vulval muscles GCaMP5, mCherry	*goa-1(sa734) I; vsIs164 lite-1(ce314) lin-15(n765ts) X*	this study
MIA331	GOA-1 ($G\alpha_o$) null mutant; EGL-4 (Protein Kinase G) null mutant	*goa-1(sa734)I; egl-4(n479)IV*	this study
MIA345	GOA-1 ($G\alpha_o$) null mutant; no HSNs	*goa-1(sa734) I; egl-1(n986dm) V*	this study
MIA359	EGL-47 null mutant; HSN GCaMP5, mCherry	*egl-47(ok677) V; vsIs183 lite-1(ce314) lin-15(n765ts) X*	this study
MIA360	NLP-7 overexpression; HSN and NSM Pertussis Toxin; HSN GCaMP5, mCherry	*ufIs118; vsIs50; vsIs186 lite-1(ce314) lin-15(n765ts) X*	this study
MIA366	NLP-7 overexpression; EGL-47 null mutant; HSN GCaMP5, mCherry	*ufIs118; egl-47(ok677) V; vsIs183 lite-1(ce314) lin-15(n765ts) X*	this study
MIA369	no HSNs; HSN and NSM Pertussis Toxin; HSN GCaMP5, mCherry	*egl-1(n986dm) V; vsIs50; vsIs186 lite-1(ce314) lin-15 (n765ts) X*	this study
MIA370	VC Tetanus Toxin; HSN and NSM Pertussis Toxin; HSN GCaMP5, mCherry	*keyIs33; vsIs186; vsIs50 keyIs33; lite-1(ce314) lin-15(n765ts) X*	this study
MIA371	GOA-1 ($G\alpha_o$) null mutant; VC Tetanus Toxin	*goa-1(sa734) I; keyIs33; lite-1(ce314) lin-15(n765ts) X*	this study
MT1073	EGL-4 (Protein Kinase G) loss-of-function mutant. Egg-laying defective, roaming locomotion	*egl-4(n478) IV*	(L'Etoile et al., 2002)
MT1074	EGL-4 (Protein Kinase G) null mutant. Egg-laying defective, roaming locomotion	*egl-4(n479) IV*	(L'Etoile et al., 2002)
MT2426	GOA-1 ($G\alpha_o$) reduced-function mutant, hyperactive egg laying	*goa-1(n1134) I*	(Segalat et al., 1995)
MT8504	Increased $G\alpha_o$ signaling due to mutation in RGS protein, EGL-10	*egl-10(md176) V*	(Koelle and Horvitz, 1996)
RB850	EGL-47 null mutant	*egl-47(ok677) V*	(Moresco and Koelle, 2004; Consortium, 2012)

1016

1017 **References**

1018 Alkema MJ, Hunter-Ensor M, Ringstad N, Horvitz HR (2005) Tyramine Functions independently of
1019 octopamine in the Caenorhabditis elegans nervous system. Neuron 46:247-260.
1020 Aprison EZ, Ruvinsky I (2014) Balanced trade-offs between alternative strategies shape the
1021 response of C. elegans reproduction to chronic heat stress. PLoS One 9:e105513.
1022 Aprison EZ, Ruvinsky I (2019a) Coordinated Behavioral and Physiological Responses to a Social
1023 Signal Are Regulated by a Shared Neuronal Circuit. Curr Biol 29:4108-4115 e4104.
1024 Aprison EZ, Ruvinsky I (2019b) Dynamic Regulation of Adult-Specific Functions of the Nervous
1025 System by Signaling from the Reproductive System. Curr Biol 29:4116-4123 e4113.
1026 Banerjee N, Bhattacharya R, Gorczyca M, Collins KM, Francis MM (2017) Local neuropeptide
1027 signaling modulates serotonergic transmission to shape the temporal organization of *C.*
1028 *elegans* egg-laying behavior. PLoS Genet 13:e1006697.
1029 Bany IA, Dong MQ, Koelle MR (2003) Genetic and cellular basis for acetylcholine inhibition of
1030 *Caenorhabditis elegans* egg-laying behavior. J Neurosci 23:8060-8069.
1031 Bastiani CA, Gharib S, Simon MI, Sternberg PW (2003) Caenorhabditis elegans Galphaq regulates
1032 egg-laying behavior via a PLCbeta-independent and serotonin-dependent signaling
1033 pathway and likely functions both in the nervous system and in muscle. Genetics 165:1805-
1034 1822.
1035 Bellemer A, Hirata T, Romero MF, Koelle MR (2011) Two types of chloride transporters are
1036 required for GABA(A) receptor-mediated inhibition in *C. elegans*. EMBO J 30:1852-1863.
1037 Borden PM et al. (2020) A fast genetically encoded fluorescent sensor for faithful in
1038 vivo acetylcholine detection in mice, fish, worms and flies.
1039 bioRxiv:2020.2002.2007.939504.
1040 Branicky R, Miyazaki H, Strange K, Schafer WR (2014) The voltage-gated anion channels encoded
1041 by clh-3 regulate egg laying in C. elegans by modulating motor neuron excitability. J
1042 Neurosci 34:764-775.
1043 Brenner S (1974) The genetics of *Caenorhabditis elegans*. Genetics 77:71-94.
1044 Brewer JC, Collins KM, Koelle MR, Olsen A (2019) Serotonin and neuropeptides are both released
1045 by the HSN command neuron to initiate C. elegans egg laying. PLoS Genet 15.
1046 Brundage L, Avery L, Katz A, Kim UJ, Mendel JE, Sternberg PW, Simon MI (1996) Mutations in a C.
1047 elegans Gqalpha gene disrupt movement, egg laying, and viability. Neuron 16:999-1009.
1048 Carnell L, Illi J, Hong SW, McIntire SL (2005) The G-protein-coupled serotonin receptor SER-1
1049 regulates egg laying and male mating behaviors in *Caenorhabditis elegans*. J Neurosci
1050 25:10671-10681.
1051 Charlie NK, Schade MA, Thomure AM, Miller KG (2006a) Presynaptic UNC-31 (CAPS) is required to
1052 activate the G alpha(s) pathway of the Caenorhabditis elegans synaptic signaling network.
1053 Genetics 172:943-961.
1054 Charlie NK, Thomure AM, Schade MA, Miller KG (2006b) The Dunce cAMP phosphodiesterase
1055 PDE-4 negatively regulates G alpha(s)-dependent and G alpha(s)-independent cAMP pools
1056 in the Caenorhabditis elegans synaptic signaling network. Genetics 173:111-130.
1057 Chase DL, Pepper JS, Koelle MR (2004) Mechanism of extrasynaptic dopamine signaling in
1058 *Caenorhabditis elegans*. Nat Neurosci 7:1096-1103.
1059 Clark SG, Lu X, Horvitz HR (1994) The Caenorhabditis elegans locus lin-15, a negative regulator of
1060 a tyrosine kinase signaling pathway, encodes two different proteins. Genetics 137:987.
1061 Collins KM, Koelle MR (2013) Postsynaptic ERG potassium channels limit muscle excitability to
1062 allow distinct egg-laying behavior states in *Caenorhabditis elegans*. J Neurosci 33:761-775.

1063 Collins KM, Bode A, Fernandez RW, Tanis JE, Brewer JC, Creamer MS, Koelle MR (2016) Activity of
1064 the *C. elegans* egg-laying behavior circuit is controlled by competing activation and
1065 feedback inhibition. Elife 5:e21126.
1066 Consortium CeDM (2012) large-scale screening for targeted knockouts in the Caenorhabditis
1067 elegans genome. G3 (Bethesda) 2:1415-1425.
1068 Crunelli V, Toth TI, Cope DW, Blethyn K, Hughes SW (2005) The 'window' T-type calcium current
1069 in brain dynamics of different behavioural states. J Physiol 562:121-129.
1070 Dempsey CM, Mackenzie SM, Gargus A, Blanco G, Sze JY (2005) Serotonin (5HT), fluoxetine,
1071 imipramine and dopamine target distinct 5HT receptor signaling to modulate
1072 *Caenorhabditis elegans* egg-laying behavior. Genetics 169:1425-1436.
1073 Dong MQ, Chase D, Patikoglou GA, Koelle MR (2000) Multiple RGS proteins alter neural G protein
1074 signaling to allow C. elegans to rapidly change behavior when fed. Genes Dev 14:2003-
1075 2014.
1076 Emtage L, Aziz-Zaman S, Padovan-Merhar O, Horvitz HR, Fang-Yen C, Ringstad N (2012) IRK-1
1077 potassium channels mediate peptidergic inhibition of *Caenorhabditis elegans* serotonin
1078 neurons via a G(o) signaling pathway. J Neurosci 32:16285-16295.
1079 Esposito G, Di Schiavi E, Bergamasco C, Bazzicalupo P (2007) Efficient and cell specific knock-
1080 down of gene function in targeted C. elegans neurons. Gene 395:170-176.
1081 Fenk LA, de Bono M (2015) Environmental CO2 inhibits Caenorhabditis elegans egg-laying by
1082 modulating olfactory neurons and evokes widespread changes in neural activity. Proc Natl
1083 Acad Sci U S A 112:E3525-3534.
1084 Fernandez RW, Wei K, Wang EY, Mikalauskaite D, Olson A, Pepper J, Christie N, Kim S, Koelle MR
1085 (2020) Cellular expression and functional roles of all 26 neurotransmitter GPCRs in the
1086 C. elegans egg-laying circuit. bioRxiv:2020.2004.2023.037242.
1087 Fujiwara M, Sengupta P, McIntire SL (2002) Regulation of body size and behavioral state of C.
1088 elegans by sensory perception and the EGL-4 cGMP-dependent protein kinase. Neuron
1089 36:1091-1102.
1090 Fujiwara M, Hino T, Miyamoto R, Inada H, Mori I, Koga M, Miyahara K, Ohshima Y, Ishihara T
1091 (2015) The Importance of cGMP Signaling in Sensory Cilia for Body Size Regulation in
1092 Caenorhabditis elegans. Genetics 201:1497-1510.
1093 Gao S, Zhen M (2011) Action potentials drive body wall muscle contractions in Caenorhabditis
1094 elegans. Proc Natl Acad Sci U S A 108:2557-2562.
1095 Garcia J, Collins KM (2019) The HSN egg-laying command neurons are required for normal
1096 defecation frequency in Caenorhabditis elegans (II). microPublication Biology.
1097 Ghil S, Choi JM, Kim SS, Lee YD, Liao Y, Birnbaumer L, Suh-Kim H (2006) Compartmentalization of
1098 protein kinase A signaling by the heterotrimeric G protein Go. Proc Natl Acad Sci U S A
1099 103:19158-19163.
1100 Goulding EH, Schenk AK, Juneja P, MacKay AW, Wade JM, Tecott LH (2008) A robust automated
1101 system elucidates mouse home cage behavioral structure. Proc Natl Acad Sci U S A
1102 105:20575-20582.
1103 Gurel G, Gustafson MA, Pepper JS, Horvitz HR, Koelle MR (2012) Receptors and other signaling
1104 proteins required for serotonin control of locomotion in *Caenorhabditis elegans*. Genetics
1105 192:1359-1371.
1106 Han B, Bellemer A, Koelle MR (2015) An evolutionarily conserved switch in response to GABA
1107 affects development and behavior of the locomotor circuit of Caenorhabditis elegans.
1108 Genetics 199:1159-1172.
1109 Hao Y, Xu N, Box AC, Schaefer L, Kannan K, Zhang Y, Florens L, Seidel C, Washburn MP, Wiegraebe
1110 W, Mak HY (2011) Nuclear cGMP-dependent kinase regulates gene expression via activity-

1111 dependent recruitment of a conserved histone deacetylase complex. PLoS Genet
1112 7:e1002065.
1113 Harfe BD, Fire A (1998) Muscle and nerve-specific regulation of a novel NK-2 class homeodomain
1114 factor in *Caenorhabditis elegans*. Development 125:421-429.
1115 Herlitze S, Garcia DE, Mackie K, Hille B, Scheuer T, Catterall WA (1996) Modulation of Ca2+
1116 channels by G-protein beta gamma subunits. Nature 380:258-262.
1117 Hille B (1994) Modulation of ion-channel function by G-protein-coupled receptors. Trends
1118 Neurosci 17:531-536.
1119 Hobson RJ, Hapiak VM, Xiao H, Buehrer KL, Komuniecki PR, Komuniecki RW (2006) SER-7, a
1120 *Caenorhabditis elegans* 5-HT7-like receptor, is essential for the 5-HT stimulation of
1121 pharyngeal pumping and egg laying. Genetics 172:159-169.
1122 Horvitz HR, Chalfie M, Trent C, Sulston JE, Evans PD (1982) Serotonin and octopamine in the
1123 nematode Caenorhabditis elegans. Science 216:1012-1014.
1124 Jansen G, Thijssen KL, Werner P, van der Horst M, Hazendonk E, Plasterk RH (1999) The complete
1125 family of genes encoding G proteins of Caenorhabditis elegans. Nat Genet 21:414-419.
1126 Jiang M, Spicher K, Boulay G, Wang Y, Birnbaumer L (2001) Most central nervous system D2
1127 dopamine receptors are coupled to their effectors by Go. Proc Natl Acad Sci U S A 98:3577-
1128 3582.
1129 Jose AM, Koelle MR (2005) Domains, amino acid residues, and new isoforms of Caenorhabditis
1130 elegans diacylglycerol kinase 1 (DGK-1) important for terminating diacylglycerol signaling
1131 in vivo. J Biol Chem 280:2730-2736.
1132 Jose AM, Bany IA, Chase DL, Koelle MR (2007) A specific subset of transient receptor potential
1133 vanilloid-type channel subunits in Caenorhabditis elegans endocrine cells function as
1134 mixed heteromers to promote neurotransmitter release. Genetics 175:93-105.
1135 Kobayashi I, Shibasaki H, Takahashi K, Tohyama K, Kurachi Y, Ito H, Ui M, Katada T (1990)
1136 Purification and characterization of five different alpha subunits of guanine-nucleotide-
1137 binding proteins in bovine brain membranes. Their physiological properties concerning the
1138 activities of adenylate cyclase and atrial muscarinic K+ channels. Eur J Biochem 191:499-
1139 506.
1140 Koelle MR (2016) Neurotransmitter signaling through heterotrimeric G proteins: insights from
1141 studies in C. elegans. WormBook:1-78.
1142 Koelle MR, Horvitz HR (1996) EGL-10 regulates G protein signaling in the C. elegans nervous
1143 system and shares a conserved domain with many mammalian proteins. Cell 84:115-125.
1144 Kwok TC, Ricker N, Fraser R, Chan AW, Burns A, Stanley EF, McCourt P, Cutler SR, Roy PJ (2006) A
1145 small-molecule screen in C. elegans yields a new calcium channel antagonist. Nature
1146 441:91-95.
1147 L'Etoile ND, Coburn CM, Eastham J, Kistler A, Gallegos G, Bargmann CI (2002) The cyclic GMP-
1148 dependent protein kinase EGL-4 regulates olfactory adaptation in C. elegans. Neuron
1149 36:1079-1089.
1150 Lackner MR, Nurrish SJ, Kaplan JM (1999) Facilitation of synaptic transmission by EGL-30 Gqalpha
1151 and EGL-8 PLCbeta: DAG binding to UNC-13 is required to stimulate acetylcholine release.
1152 Neuron 24:335-346.
1153 Lee RY, Lobel L, Hengartner M, Horvitz HR, Avery L (1997) Mutations in the alpha1 subunit of an
1154 L-type voltage-activated Ca2+ channel cause myotonia in Caenorhabditis elegans. EMBO J
1155 16:6066-6076.
1156 Li P, Collins KM, Koelle MR, Shen K (2013) LIN-12/Notch signaling instructs postsynaptic muscle
1157 arm development by regulating UNC-40/DCC and MADD-2 in *Caenorhabditis elegans*. Elife
1158 2:e00378.

1159 Liu P, Ge Q, Chen B, Salkoff L, Kotlikoff MI, Wang ZW (2011) Genetic dissection of ion currents
1160 underlying all-or-none action potentials in C. elegans body-wall muscle cells. J Physiol
1161 589:101-117.
1162 Liu Q, Kidd PB, Dobosiewicz M, Bargmann CI (2018) C. elegans AWA Olfactory Neurons Fire
1163 Calcium-Mediated All-or-None Action Potentials. Cell 175:57-70 e17.
1164 Lou X, Korogod N, Brose N, Schneggenburger R (2008) Phorbol esters modulate spontaneous and
1165 Ca2+-evoked transmitter release via acting on both Munc13 and protein kinase C. J
1166 Neurosci 28:8257-8267.
1167 Lu B, Su Y, Das S, Wang H, Wang Y, Liu J, Ren D (2009) Peptide neurotransmitters activate a cation
1168 channel complex of NALCN and UNC-80. Nature 457:741-744.
1169 Lutas A, Lahmann C, Soumillon M, Yellen G (2016) The leak channel NALCN controls tonic firing
1170 and glycolytic sensitivity of substantia nigra pars reticulata neurons. Elife 5.
1171 Marder E (2012) Neuromodulation of neuronal circuits: back to the future. Neuron 76:1-11.
1172 Mathews EA, Garcia E, Santi CM, Mullen GP, Thacker C, Moerman DG, Snutch TP (2003) Critical
1173 residues of the Caenorhabditis elegans unc-2 voltage-gated calcium channel that affect
1174 behavioral and physiological properties. J Neurosci 23:6537-6545.
1175 Matsubara H (2002) [Angiotensin II type 2 (AT2) receptor signal and cardiovascular action].
1176 Nihon Yakurigaku Zasshi 119:95-102.
1177 McMullan R, Nurrish SJ (2011) The RHO-1 RhoGTPase modulates fertility and multiple behaviors
1178 in adult C. elegans. PLoS One 6:e17265.
1179 McMullan R, Hiley E, Morrison P, Nurrish SJ (2006) Rho is a presynaptic activator of
1180 neurotransmitter release at pre-existing synapses in C. elegans. Genes Dev 20:65-76.
1181 McMullen PD, Aprison EZ, Winter PB, Amaral LA, Morimoto RI, Ruvinsky I (2012) Macro-level
1182 modeling of the response of C. elegans reproduction to chronic heat stress. PLoS Comput
1183 Biol 8:e1002338.
1184 Mendel JE, Korswagen HC, Liu KS, Hajdu-Cronin YM, Simon MI, Plasterk RH, Sternberg PW (1995)
1185 Participation of the protein Go in multiple aspects of behavior in C. elegans. Science
1186 267:1652-1655.
1187 Miller KG, Emerson MD, Rand JB (1999) Goalpha and diacylglycerol kinase negatively regulate the
1188 Gqalpha pathway in C. elegans. Neuron 24:323-333.
1189 Mitchell DH, Stiles JW, Santelli J, Sanadi DR (1979) Synchronous growth and aging of
1190 Caenorhabditis elegans in the presence of fluorodeoxyuridine. J Gerontol 34:28-36.
1191 Moresco JJ, Koelle MR (2004) Activation of EGL-47, a Galpha(o)-coupled receptor, inhibits function
1192 of hermaphrodite-specific motor neurons to regulate *Caenorhabditis elegans* egg-laying
1193 behavior. J Neurosci 24:8522-8530.
1194 Mumby SM, Heukeroth RO, Gordon JI, Gilman AG (1990) G-protein alpha-subunit expression,
1195 myristoylation, and membrane association in COS cells. Proc Natl Acad Sci U S A 87:728-
1196 732.
1197 Nurrish S, Segalat L, Kaplan JM (1999) Serotonin inhibition of synaptic transmission: Galpha(0)
1198 decreases the abundance of UNC-13 at release sites. Neuron 24:231-242.
1199 Pan B, Akyuz N, Liu XP, Asai Y, Nist-Lund C, Kurima K, Derfler BH, Gyorgy B, Limapichat W,
1200 Walujkar S, Wimalasena LN, Sotomayor M, Corey DP, Holt JR (2018) TMC1 Forms the Pore
1201 of Mechanosensory Transduction Channels in Vertebrate Inner Ear Hair Cells. Neuron
1202 99:736-753 e736.
1203 Philippart F, Khaliq ZM (2018) Gi/o protein-coupled receptors in dopamine neurons inhibit the
1204 sodium leak channel NALCN. Elife 7.

1205 Raizen DM, Cullison KM, Pack AI, Sundaram MV (2006) A novel gain-of-function mutant of the
1206 cyclic GMP-dependent protein kinase egl-4 affects multiple physiological processes in
1207 Caenorhabditis elegans. Genetics 173:177-187.
1208 Ravi B, Garcia J, Collins KM (2018a) Homeostatic feedback modulates the development of two-
1209 state patterned activity in a model serotonin motor circuit in Caenorhabditis elegans. J
1210 Neurosci 38:6283-6298.
1211 Ravi B, Nassar LM, Kopchock RJ, 3rd, Dhakal P, Scheetz M, Collins KM (2018b) Ratiometric calcium
1212 imaging of individual neurons in behaving Caenorhabditis elegans. J Vis Exp.
1213 Reuveny E, Slesinger PA, Inglese J, Morales JM, Iniguez-Lluhi JA, Lefkowitz RJ, Bourne HR, Jan YN,
1214 Jan LY (1994) Activation of the cloned muscarinic potassium channel by G protein beta
1215 gamma subunits. Nature 370:143-146.
1216 Reynolds NK, Schade MA, Miller KG (2005) Convergent, RIC-8-dependent Galpha signaling
1217 pathways in the Caenorhabditis elegans synaptic signaling network. Genetics 169:651-670.
1218 Ringstad N, Horvitz HR (2008) FMRFamide neuropeptides and acetylcholine synergistically inhibit
1219 egg-laying by *C. elegans*. Nat Neurosci 11:1168-1176.
1220 Robatzek M, Thomas JH (2000) Calcium/calmodulin-dependent protein kinase II regulates
1221 Caenorhabditis elegans locomotion in concert with a G(o)/G(q) signaling network. Genetics
1222 156:1069-1082.
1223 Sawin ER (1996) Genetic and Cellular Analysis of Modulated Behaviors in Caenorhabditis elegans.
1224 In, p 316: Massachusetts Institute of Technology, Cambridge, USA.
1225 Schade MA, Reynolds NK, Dollins CM, Miller KG (2005) Mutations that rescue the paralysis of
1226 Caenorhabditis elegans ric-8 (synembryn) mutants activate the G alpha(s) pathway and
1227 define a third major branch of the synaptic signaling network. Genetics 169:631-649.
1228 Schafer WF (2006) Genetics of egg-laying in worms. Annu Rev Genet 40:487-509.
1229 Schafer WR, Kenyon CJ (1995) A calcium-channel homologue required for adaptation to dopamine
1230 and serotonin in Caenorhabditis elegans. Nature 375:73-78.
1231 Segalat L, Elkes DA, Kaplan JM (1995) Modulation of serotonin-controlled behaviors by Go in
1232 *Caenorhabditis elegans*. Science 267:1648-1651.
1233 Shen K, Fetter RD, Bargmann CI (2004) Synaptic specificity is generated by the synaptic guidepost
1234 protein SYG-2 and its receptor, SYG-1. Cell 116:869-881.
1235 Shyn SI, Kerr R, Schafer WR (2003) Serotonin and Go modulate functional states of neurons and
1236 muscles controlling C. elegans egg-laying behavior. Curr Biol 13:1910-1915.
1237 Tang YQ, Lee SA, Rahman M, Vanapalli SA, Lu H, Schafer WR (2020) Ankyrin Is An Intracellular
1238 Tether for TMC Mechanotransduction Channels. Neuron.
1239 Tanis JE, Moresco JJ, Lindquist RA, Koelle MR (2008) Regulation of serotonin biosynthesis by the G
1240 proteins Galphao and Galphaq controls serotonin signaling in *Caenorhabditis elegans*.
1241 Genetics 178:157-169.
1242 Tanis JE, Bellemer A, Moresco JJ, Forbush B, Koelle MR (2009) The potassium chloride
1243 cotransporter KCC-2 coordinates development of inhibitory neurotransmission and
1244 synapse structure in *Caenorhabditis elegans*. J Neurosci 29:9943-9954.
1245 Topalidou I, Cooper K, Pereira L, Ailion M (2017a) Dopamine negatively modulates the NCA ion
1246 channels in C. elegans. PLoS Genet 13:e1007032.
1247 Topalidou I, Chen PA, Cooper K, Watanabe S, Jorgensen EM, Ailion M (2017b) The NCA-1 and NCA-
1248 2 Ion Channels Function Downstream of Gq and Rho To Regulate Locomotion in
1249 Caenorhabditis elegans. Genetics 206:265-282.
1250 Trent C (1982) Genetic and Behavioral Studies of the Egg-Laying System of *Caenorhabditis elegans*.
1251 Massachusetts Institute of Technology, Cambridge, USA.

1252 Trent C, Tsuing N, Horvitz HR (1983) Egg-laying defective mutants of the nematode
1253 Caenorhabditis elegans. Genetics 104:619-647.
1254 Waggoner LE, Zhou GT, Schafer RW, Schafer WR (1998) Control of alternative behavioral states by
1255 serotonin in *Caenorhabditis elegans*. Neuron 21:203-214.
1256 Waggoner LE, Hardaker LA, Golik S, Schafer WR (2000) Effect of a neuropeptide gene on
1257 behavioral states in Caenorhabditis elegans egg-laying. Genetics 154:1181-1192.
1258 White JG, Southgate E, Thomson JN, Brenner S (1986) The structure of the nervous system of the
1259 nematode *Caenorhabditis elegans*. Philos Trans R Soc Lond B Biol Sci 314:1-340.
1260 Wierda KD, Toonen RF, de Wit H, Brussaard AB, Verhage M (2007) Interdependence of PKC-
1261 dependent and PKC-independent pathways for presynaptic plasticity. Neuron 54:275-290.
1262 Williams SL, Lutz S, Charlie NK, Vettel C, Ailion M, Coco C, Tesmer JJ, Jorgensen EM, Wieland T,
1263 Miller KG (2007) Trio's Rho-specific GEF domain is the missing Galpha q effector in C.
1264 elegans. Genes Dev 21:2731-2746.
1265 Williams SR, Toth TI, Turner JP, Hughes SW, Crunelli V (1997) The 'window' component of the low
1266 threshold Ca2+ current produces input signal amplification and bistability in cat and rat
1267 thalamocortical neurones. J Physiol 505 (Pt 3):689-705.
1268 Yamada K, Hirotsu T, Matsuki M, Kunitomo H, Iino Y (2009) GPC-1, a G protein gamma-subunit,
1269 regulates olfactory adaptation in Caenorhabditis elegans. Genetics 181:1347-1357.
1270 Yawo H (1999) Protein kinase C potentiates transmitter release from the chick ciliary presynaptic
1271 terminal by increasing the exocytotic fusion probability. J Physiol 515 (Pt 1):169-180.
1272 Yeh E, Ng S, Zhang M, Bouhours M, Wang Y, Wang M, Hung W, Aoyagi K, Melnik-Martinez K, Li M,
1273 Liu F, Schafer WR, Zhen M (2008) A putative cation channel, NCA-1, and a novel protein,
1274 UNC-80, transmit neuronal activity in C. elegans. PLoS Biol 6:e55.
1275 Yue X, Zhao J, Li X, Fan Y, Duan D, Zhang X, Zou W, Sheng Y, Zhang T, Yang Q, Luo J, Duan S, Xiao R,
1276 Kang L (2018) TMC Proteins Modulate Egg Laying and Membrane Excitability through a
1277 Background Leak Conductance in C. elegans. Neuron 97:571-585 e575.
1278 Zang KE, Ho E, Ringstad N (2017) Inhibitory peptidergic modulation of *C. elegans* serotonin
1279 neurons is gated by T-type calcium channels. Elife 6:e22771.
1280 Zhang J, Pratt RE (1996) The AT2 receptor selectively associates with Gialpha2 and Gialpha3 in
1281 the rat fetus. J Biol Chem 271:15026-15033.
1282 Zhang M, Chung SH, Fang-Yen C, Craig C, Kerr RA, Suzuki H, Samuel AD, Mazur E, Schafer WR
1283 (2008) A self-regulating feed-forward circuit controlling C. elegans egg-laying behavior.
1284 Curr Biol 18:1445-1455.
1285 Zou W, Fu J, Zhang H, Du K, Huang W, Yu J, Li S, Fan Y, Baylis HA, Gao S, Xiao R, Ji W, Kang L, Xu T
1286 (2018) Decoding the intensity of sensory input by two glutamate receptors in one C.
1287 elegans interneuron. Nat Commun 9:4311.

1288